Geochemical and Microbiological Characterization of the Arbuckle Saline Aquifer, a Potential CO_2 Storage Reservoir; Implications for Hydraulic Separation and Caprock Integrity

BY

Aimee Scheffer

B.S., University of Colorado

M.S., University of Arkansas

Submitted to the graduate degree program in Geology and the Graduate Faculty of the University of Kansas in partial fulfillment of the requirements for the degree of Master of Science.

Advisory Committee:

Dr. Jennifer A. Roberts_____
Committee chair

Dr. W. Lynn Watney_____

Dr. David A. Fowle_____

Date Approved: _____

Date Submitted: _____

The Thesis Committee for Aimee Scheffer certifies that this is the approved version of the following thesis:

Geochemical and Microbiological Characterization of the Arbuckle Saline Aquifer, a Potential CO_2 Storage Reservoir; Implications for Hydraulic Separation and Caprock Integrity

Advisory Committee:

Dr. Jennifer A. Roberts_____
Committee chair

Dr. W. Lynn Watney_____

Dr. David A. Fowle_____

Date Approved: _____

Date Submitted: _____

Abstract

Aimee Scheffer
Department of Geology, July 2012
University of Kansas

Due to the mounting concern about climate change, geologic carbon storage (GCS) has become an attractive method of reducing atmospheric carbon. The United States has set ambitious goals for decreasing their CO_2 emissions and in order to meet those goals, implementation of GCS is almost certainly necessary. As a result, the Department of Energy has funded the examination of the Arbuckle saline aquifer, as well as other aquifers around the United States, to assess their potential as carbon storage sites. Geologic sequestration of CO_2 has been shown to be a feasible option, but research into details of CO_2 storage is still needed. The Arbuckle is a deep (approximately 1270-meters below land surface), saline aquifer located in south-central Kansas. This study used geological, geochemical, and microbiological data combined with laboratory experimentation to examine the reservoir connectivity and caprock integrity of the Arbuckle saline aquifer using materials from two cores collected in the Wellington oil field in Sumner County, Kansas.

Results from field characterization present strong evidence of hydraulic separation of the Upper and Lower Arbuckle and the likelihood of an extensive fracture network evidenced by essentially homogeneous brines in the Lower Arbuckle. Hydraulic separation of the Upper and Lower Arbuckle could result in decreased storage capacity, however isotopic data also points toward the presence of smaller, less influential baffles

in the Upper Arbuckle which could serve as important impediments to buoyant plume behavior, increasing pore space and solubility trapping.

Controlled, laboratory batch experiments carried out as part of this study also produced results with interesting implications for injectivity and caprock integrity of the Arbuckle aquifer. These experiments utilized the Chattanooga Shale, the immediate seal for the Arbuckle, the Cherokee Shale, the regional seal, and dolomite, the most abundant mineral in the storage reservoir. Gypsum precipitation occurred when the Chattanooga Shale containing pyrite was exposed to 100% pCO_2. Similarly, gypsum precipitation and rhomboclase dissolution occurred when pure pyrite was exposed to 100% pCO_2. Dissolution of the dolomite was the predominant reaction for the dolomite experiments. Although XRD did not detect bulk mineralogic changes in Cherokee Shale experiments decreases in iron, increases in magnesium, and decreases in calcium indicate reactions with the Cherokee Shale *are* occurring. Results indicate that precipitation of secondary gypsum will occur when Arbuckle rocks containing pyrite are exposed to CO_2.

These results have important implications for GCS in the Arbuckle saline aquifer. Hydraulic separation of the Upper and Lower Arbuckle will positively impact the plume movement in the reservoir, retarding buoyant flow. This is important because the data also show that the Lower Arbuckle brines are relatively homogenous and undergoing rapid mixing due to an extensive fracture network suggesting the plume will travel relatively quickly to the central baffle. Furthermore, the separation impacts storage capacity estimates because the tight nature of the rock that is causing the hydraulic separation is not likely to receive volumes of CO_2 equivalent to other parts of the reservoir. Additionally, if CO_2 is not able to pass through the baffle to fill the shallower

pore space within tens or hundreds of years (however long humans are injecting) then it effectively removes that volume of storage from capacity unless CO_2 is injected separately into each zone. The results of the caprock integrity study also have important implications for GCS in the Arbuckle saline aquifer. The precipitation of gypsum caused by the presence of pyrite in the reservoir will positively impact the seal integrity by beneficially filling pore space or fractures in seals resulting in even better sealing of the reservoir. However, the reservoir rocks also contain pyrite, which could also lead to gypsum precipitation, which would detrimentally clog valuable pore space in the CO_2 storage reservoir, lowering storage capacity, or decreasing injection capability.

Acknowledgments

I thank Jason Bruns of Berexco LLC, Mark Villarreal and Breanna Huff of the University of Kansas for their assistance in the field, Masato Ueshima for assistance with cation and anion analyses, Greg Kane of Keck Paleo-Environmental Stable Isotope Laboratory for preparation of reference samples used in isotopic analyses. I thank Dr. Randy Stotler for his help running oxygen and deuterium isotopes and interpretation of the data. I also thank Dr. Don Whittemore for his help with interpretation of bromine and chlorine ratios.

The research discussed in Chapter 4 and Appendix B of this thesis was supported by the U.S. Department of Energy (DOE) and was supported in part by an appointment to the National Energy Technology Laboratory Research Participation Program, sponsored by the U.S. Department of Energy and administered by the Oak Ridge Institute for Science and Education (ORISE). This research was also funded by the Kansas Geological Survey, DOSECC, Rocky Mountain Federation of Mineralogic Societies, Kansas Geological Society, and the Association for Women Geoscientists.

Material presented is based upon work supported by the U.S. Department of Energy (DOE) National Energy Technology Laboratory (NETL) under Grant Number DEFE0000002056. This project is managed and administered by the Kansas Geological Survey/KUCR, W. L. Watney, PI, and funded by DOE/NETL and cost-sharing partners.

of any information, apparatus, product, or process disclosed, or represents that its use would not infringe privately owned rights. Reference herein to any specific commercial product, process, or service by trade name, trademark, manufacturer, or otherwise does not necessarily constitute or imply its endorsement, recommendation, or favoring by the United States Government or any agency thereof. The views and opinions of authors expressed herein do not necessarily state or reflect those of the United States Government or any agency thereof.

Table of Contents

List of Figures: viii
List of Equations: ix
List of Tables: ..... **Error! Bookmark not defined.**
List of Appendices ..... **Error! Bookmark not defined.**

List of Figures:

Figure 1.1:……..……..……...2
Figure 2.1:……..……..……13
Figure 2.2:……..……..……14
Figure 2.3:……..……..……17
Figure 3.1:……..……..……23
Figure 3.2:……..……..……31
Figure 3.3:……..……..……33
Figure 3.4:……..……..……35
Figure 3.5:……..……..……36
Figure 3.6:……..……..……39
Figure 3.7:……..……..……40
Figure 4.1:……..……..……54
Figure 4.2:……..……..……60
Figure 4.3:……..……..……62
Figure 4.4:……..……..……63

List of Tables:

Table 2.1:……..……..……14
Table 4.1:……..……..……53
Table 4.2:……..……..……55
Table 4.3:……..……..……56
Table 4.4:……..……..……61
Table 4.5:……..……..……62
Table 4.6:……..……..……65

List of Equations:

Equation 1.1:……4
Equation 1.2:……..4
Equation 1.3:……...4
Equation 1.4:……..4
Equation 1.5:……4
Equation 1.6:……..4
Equation 4.1:……58
Equation 4.2:……..58
Equation 4.3:……58

List of Appendices:

Appendix Table A.1:……70
Appendix Table A.2:……70
Appendix Table A.3:……71
Appendix Table B.1:……73
Appendix Figure B.1:……73
Appendix Table B.2:……73
Appendix Figure B.2:……74
Appendix Figure B.3:……75
Appendix Figure B.4:……75
Appendix Figure B.5:……76
Appendix Figure B.6:……76
Appendix Figure B.7:……77
Appendix Figure B.8:……77
Appendix Figure B.9:……78
Appendix Figure B.10:……78
Appendix Figure B.11:……79
Appendix Figure C.1:……80
Appendix Figure C.2:……80

Appendix Figure C.3:…..……..……81
Appendix Figure C.4:…..……..……81
Appendix Table D.1:……...……..……82
Appendix Table D.2:……...……..……83
Appendix Table D.3:……...……..……83

CHAPTER 1
INTRODUCTION

This study used geologic, geochemical, and microbiological data to examine the reservoir connectivity and caprock integrity of the Arbuckle saline aquifer in south-central Kansas. The Arbuckle is a potential CO_2 storage reservoir and will receive 40,000 tonnes of CO_2 during a 2013 pilot CO_2 injection in Wellington oil field in Sumner County, Kansas.

Increased concentrations of greenhouse gases in the atmosphere, such as carbon dioxide (CO_2), contribute to global warming. Anthropogenic consumption of fossil fuels is increasing the concentration of CO_2 at a rate of approximately 1 ppm annually (www.iea.org/statistics). Therefore, there is great interest in both reducing CO_2 emissions and capturing and storing CO_2 underground by geological carbon storage (GCS). Carbon dioxide can be sequestered for tens of thousands to millions of years in geological formations by pore space trapping of CO_2 gas, dissolution into the brine, and by in-situ precipitation through mineral carbonation (Gunter et al., 1996). Each potential storage site has unique geology and will come with a distinctive set of challenges that need to be evaluated. The pressure and temperature conditions of most saline aquifers, including the Arbuckle saline aquifer, require the carbon dioxide to be injected as a supercritical fluid.

Supercritical carbon dioxide ($CO_{2(sc)}$)

Super critical fluids are utilized in many diverse industrial applications. The primary use of supercritical carbon dioxide ($CO_{2(sc)}$) is chemical extractions such as the decaffeination of coffee and tea (Mohamed and Saldana, 2002) but it is also routinely used by the food industry to prevent food spoilage, although sterilization is rarely achieved (Dixon et al., 1989). $CO_{2(sc)}$ has unique properties which cause a decrease in the surface tension of fluids and enables mixtures to move freely in small pores (Brunner, 2010). These properties have proved useful in the field of

enhanced oil recovery. Carbon dioxide will be in a supercritical state at in-situ temperatures above 87° F and pressures above 1200 psi (Fig. 1), conditions which are met by most saline aquifers (Daneshfar et al., 2009).

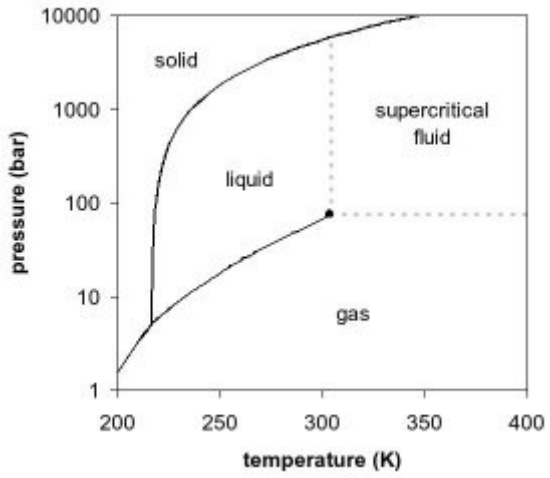

Figure 1.1 Phase diagram for CO_2. "Supercritical fluid." *New World Encyclopedia,* . 2 Apr 2008, 17:14 UTC. 4 Jul 2012, 23:44 <http://www.newworldencyclopedia.org/p/index.php?title=Supercritical_fluid&oldid=683499>.

Geochemistry

CO_2 is highly reactive and the geochemical interactions in the reservoir are complex. Initially, CO_2 concentration is highest near the point of injection and gradually decreases with distance from the injection well. This variation in concentration and pressure will manifest in a series of variable reaction rates as the system works to achieve equilibrium with the saturation states of minerals, CO_2 concentration, and pH of the reservoir fluid. In the near-wellbore region, non-equilibrium geochemical reactions are likely to occur, whereas in the distant regions, a system closer to equilibrium is likely (Egermann et al., 2010; Luquot, 2009).

Carbon dioxide can be stored in four different modes: (1) as a separate supercritical phase; (2) as trapped gas; (3) dissolved in the aqueous phase; and (4) as solid minerals (Metz, 2005). First, the CO_2 will dissolve in the water, acidifying it, called solubility trapping, then it will form ionic species as the host rock dissolves accompanied by a rise in the pH and finally

some fraction of the CO_2 may be converted to stable mineral phases such as carbonate minerals (Hitchon, 1999). Ionic trapping, as HCO_3^-, is short-term (<50 year) and can be quantified using chemical and isotopic techniques outlined by Raistrick et al. (2006). The integrity of the structural traps, cap rocks and stratigraphy of the storage formation are particularly important for the gaseous and aqueous phases of CO_2. Different methods of CO_2 storage vary depending on reaction rates with the mineral composition of the aquifer, and therefore the storage capability of each trapping mechanism will vary from site to site.

The extent of pore space trapping of CO_2 gas depends on the characteristics of the rock making up the aquifer (Kumar et al., 2004). At the water-CO_2 interface, dissolution of the CO_2 into water will start to occur. In general, pore space trapping and dissolving CO_2 into the aqueous phase are the most desirable outcomes and take increasing amounts of time. Solubility trapping involves the dissolution of CO_2 into a fluid phase, including both aqueous brines and oil and can occur at fast rates (Lin et al., 2007). Migrating plume into tighter rock with smaller pore space would help degrade the plume and help minimize the free phase buildup beneath the caprock. Carbon dioxide trapping reactions are expected to take 100s of years to complete (Gunter and Wiwehar, 1997). Several conditions can increase the solubility of CO_2 into water and increase storage potential of a reservoir including warmer basin water (Alkan et al., 2009), density driven convection (Kneafsey et at., 2008), buoyancy-driven convection (Farajzadeh, 2009), decreased salinity brine (Alkan et al., 2009; Rimmele et al., 2008, Daneshfar et al., 2009), and increased pressures (Lin et al., 2008).

Mineral trapping involves CO_2 enriched reservoir fluids reacting with dissolved cations to precipitate carbonate minerals (Lin et al., 2008). Silicate dissolution is also expected but the focus is typically on carbonates because of the faster kinetics of the reactions. Trapping capacity

by mineral carbonation tends to be higher when solution Ca^{2+}, Mg^{2+}, and Fe^{2+}concentrations are higher (Oelkers et al., 2008) which facilitate the mineralization of carbonate minerals such as calcite ($CaCO_3$), dolomite ($CaMg(CO_3)_2$, siderite ($FeCO_3$), or magnesite ($MgCO_3$). The pathways for the formation of these minerals, respectively:

$$CO_{2\,(aq)} + H_2O \longrightarrow H_2CO_3 \qquad \text{(Equation 1.1)}$$

$$H_2CO_3 + CaCO_3\,(s) \longrightarrow Ca^{2+}_{(aq)} + 2HCO_{3(aq)} \qquad \text{(Equation 1.2)}$$

$$Ca^{2+} + CO_{2(g)} + H_2O \longrightarrow CaCO_{3\,(s)} + 2H^+ \qquad \text{(Equation 1.3)}$$

$$Ca^{2+} + Mg^{2+} + CO_{2(g)} + H_2O \longrightarrow CaMg(CO_3)_{2\,(s)} + 4H^+ \qquad \text{(Equation 1.4)}$$

$$Fe^{2+} + CO_{2(g)} + H_2O \longrightarrow FeCO_{3\,(s)} + 2H^+ \qquad \text{(Equation 1.5)}$$

$$Mg^{2+} + CO_{2(g)} + H_2O \longrightarrow MgCO_{3\,(s)} + 2H^+ \qquad \text{(Equation 1.6)}$$

It is important to note that the vast majority of the published research reported both precipitation and dissolution reactions occurring simultaneously which indicates complex geochemical interactions are occurring. For example, the study by Lu et al., 2011) indicates silicate dissolution as the dominant reaction when CO_2 is reacted with the Navajo sandstone with illite, smectite, allophane and carbonate minerals produced. It is necessary to understand these processes in order to determine to what extent and at what distances and timeframes these reactions will occur. Premature precipitation can lead to clogging of the well materials or of the aquifer itself near injection. On the other hand, rapid dissolution can lead to storage integrity concerns with well bores, well cements and cap rocks. Shales are most commonly selected as reservoir seals. Experiments by Kaszuba et al. (2003) showed shales actively participate in fluid-rock interactions in CO_2 storage systems, which shows the necessity to test caprock reactivity with CO_2 and overall integrity for each site.

In this thesis I carried out a detailed baseline geochemical characterization for the Arbuckle aquifer, the results of which are presented in Chapter 3. The changes that occurred in the brine chemistry after CO_2 exposure in a series of batch experiments with reservoir seals and brine at in situ temperatures and pressures are reported in Chapter 4.

Subsurface Microbiology

The existing research by the GCS community discussed above has largely ignored the potential influence of subsurface microbial populations on precipitation and dissolution reactions. In addition to strictly geochemical reactions, microbial processes are also known to impact carbonate mineral equilibria by altering the fluid composition, pH, concentration of elements and alteration of organic compounds (Shock, 2009) and through the production of chelating agents (Park et al., 2009). Many researchers now think that many low-temperature geochemical processes that were previously thought to be abiotic, may actually be microbially mediated (Shock, 2009). Microorganisms affect many geochemical processes because of their ability to harvest energy from a myriad of oxidation and reduction reactions through varied metabolisms (Croal et al., 2004). Microorganisms have been shown to serve as catalysts for certain geochemical reactions. Experiments conducted by Roberts et al. (2004) showed that microbial processes are the key to the formation of low-temperature dolomite after dolomite failed to precipitate in sterile experiments. Experiments by Jacobson et al. (2009) showed dissolution rates of calcite doubled in the presence of microbes. In contrast, work by Luttge and Conrad (2004) concluded that the presence of microbes actually led to a significant inhibition of the rate of calcite dissolution. The inhibition was the result of *Shewanella oneidensis* surface colonization, which inhibited the formation of etch pits. Edwards and Rutenberg (2001) showed that small local surface alterations impact the surface adhesion of microorganisms, which in turn

affects the rates of dissolution. Differences in surface micro topography between abiotic and biotic systems was also noted by Warren et al. (2001). These discrepancies highlight the complexity that should be expected of subsurface environments being considered for geologic storage of carbon. Microbial metabolism can impact dissolution and precipitation within the reservoir while microbial biomass may lead to clogging of small pores both of which affect storage capacity, injectivity, and wellbore and caprock integrity. Considering the effects of subsurface microorganisms on this already complex water:rock:CO_2 system provides for a more appropriate assessment of the system.

Detailed baseline molecular and physiological microbiological characterizations were carried out for the Arbuckle aquifer and results are presented in Chapter 3. The effects on the biomass concentrations after CO_2 exposure in a series of batch experiments with reservoir seals and brine at in situ temperatures and pressures are reported in Chapter 4.

Caprock integrity and Reservoir Connectivity

Caprock integrity of the Arbuckle saline aquifer is addressed in Chapters 3 and 4. Chapter 3 reports on a series of experiments that exposed powdered caprock materials and reservoir fluids to supercritical CO_2 at reservoir temperatures and pressures. The results are an important step in the assessment of caprock integrity. Dissolution of seal materials could allow CO_2 to breach the caprock. Preferential dissolution of fracture fill minerals is another pathway for leakage. Hence, the reactivity of the caprock and fracture fill materials with CO_2 was examined. Both the primary and secondary seals of the Arbuckle saline aquifer were explored experimentally in this study.

In addition to dissolution, another process possibly causing breach of the reservoir seal is fracturing. Chemical reactions cause volume changes, increasing stresses and potentially

fracturing the rocks. Volume changes that occur as a result of carbonation reactions can increase stress within in the rock and lead to fracturing of the rock. These fractures may then enhance transport of the mobile phase, enhancing transport of CO_2 through the rock, and accelerating the weathering process (Rudge et al., 2010). However, unintentional fracturing of the cap rock units could lead to catastrophic release of brine into drinking water sources. This is also of concern because existing unknown fractures or faults may already exist in the cap rock layers.

In this study I performed a series of 4 experiments using core materials collected from core collected in Sumner County, Kansas to examine the effects on CO_2 saturated brine on to explore the effects on potential fractures formed in the caprocks by processes discussed above. Biotic and abiotic experiments were run at reservoir temperatures (50 ºC) and pressures (2000-2500 psi). pH was monitored during the run and samples of effluent were collected every hour for cation, anion analyses throughout the experiments to measure reaction progress via inductively coupled plasma (ICP-OES), ion chromatography, respectively.

The impending pilot injection of CO_2 into the Arbuckle saline aquifer (2013) necessitated baseline geochemical and microbiologic characterization, which allowed for unique examination of reservoir connectivity. Geological investigations of the Arbuckle Group by Franseen et al., (2004), Carr et al. (1986) and others have demonstrated that the Arbuckle Group is both laterally and vertically heterogeneous. This study aimed to explore the extent and relevance of that heterogeneity to the application of carbon storage, through SC-CO_2 injection into a high-permeability zone near the base of the Arbuckle aquifer in Kansas and we present evidence of flow baffles created by discontinuous aquitards and assess the extent of isolation by regional and local aquitards in Chapter 3.

Implications

The results of this study have several implications for carbon sequestration in the Arbuckle aquifer in southern Kansas. The most profound of which is the strong evidence presented for hydraulic separation of the Upper and Lower Arbuckle, which could result in a decrease in storage capacity estimates. I also present evidence of rapid brine mixing, probably due to an extensive fracture network, in the Lower Arbuckle evidenced by essentially homogeneous brines in the Lower Arbuckle. The implications of which could affect injection and decrease rates of pore space and solubility trapping in the Lower Arbuckle. This will be evaluated by simulation of a dual porosity system. Fractures may connect the layered matrix porosity system improving contact with what seismically suggest a pods or lenses of pore space that may not be laterally continuous.

Batch experiment done for this study also produced results with interesting implications for caprock integrity and possibly injectivity of the Arbuckle aquifer. Geochemical analyses of the brine indicated mineralogic changes occurred when both the Chattanooga and Cherokee shales were exposed to 100% pCO_2. Our results indicate that precipitation of secondary gypsum will occur when Arbuckle rocks containing pyrite are exposed to CO_2. This could either beneficially fill pore space and fractures in reservoir seals, resulting in even better sealing of the reservoir, or it could detrimentally clog valuable pore space in the CO_2 storage reservoir, lowing storage capacity, or decreasing injection capability.

References

Alkan, H., Y. Cinar, and E. B. Ulker, (2010) Impact of Capillary Pressure, Salinity and In situ Conditions on CO_2 Injection into Saline Aquifers. Transport in Porous Media, 84, 3: 799-819.

Brunner, G. (2010). Applications of Supercritical Fluids. Annual Review of Chemical and Biomolecular Engineering 1, 1: 321-342.

Carr, J.E., McGovern, H. E., Gogel, T., (1986). Geohydrology of and potential for fluid disposal in the Arbuckle Aquifer in Kansas. U.S. Geological Survey open-file report, 86-491: 87.

"CO_2 Emissions from fuel combustion" (2011). International Energy Agency, 134 p., http://www.iea.org/publications/free_new_Desc.asp?PUBS_ID=2450

Croal, L.R., (2004) The genetics of geochemistry. Annual Review of Genetics. 38: 175-202.

Daneshfar, J., Hughes, R.G. and Civan, F., (2009) Feasibility Investigation and Modeling Analysis of CO_2 Sequestration in Arbuckle Formation Utilizing Salt Water Disposal Wells. Journal of Energy Resources Technology-Transactions of the Asme. 131, 2.

Dixon, N. M. and Kell, D. B. (1989). The inhibition by CO_2 of the growth and metabolism of microorganisms. Journal of Applied Bacteriology 67, 2: 109-136.

Edwards, K. J. and Rutenberg, A. D. (2001). Microbial response to surface microtopography: the role of metabolism in localized mineral dissolution. Chemical Geology 180, 1-4: 19-32.

Egermann, P., Bekri, S. (2010). An Integrated Approach to Assess the Petrophysical Properties of Rocks Altered by Rock-Fluid Interactions (CO_2 Injection). Petrophysics 51, 1: 32-40.

Farajzadeh, R., Zitha, P. L. J. (2009). Enhanced Mass Transfer of CO_2 into Water: Experiment and Modeling. Industrial & Engineering Chemistry Research 48, 13: 6423-6431.

Franseen, E.K., Byrnes, A. P. (2004). The geology of Kansas: Arbuckle Group. Kansas Geological Survey Bulletin. 250, 2: 43.

Gunter, W. D., Bachu, S. (1996). Technical and economic feasibility of CO_2 disposal in aquifers within the Alberta Sedimentary Basin, Canada. Energy Conversion and Management 37, 6-8: 1135-1142.

Gunter, W. D., Wiwehar B. (1997). Aquifer disposal of CO_2-rich greenhouse gases: Extension of the time scale of experiment for CO_2-sequestering reactions by geochemical modelling. Mineralogy and Petrology 59, 1: 121-140.

Hitchon, B., Gunter, W. D. (1999). Sedimentary basins and greenhouse gases: a serendipitous association. Energy Conversion and Management 40, 8: 825-843.

Jacobson, A. D. and Wu, L. L. (2009). Microbial dissolution of calcite at T=28 degrees C and ambient pCO_2. Geochimica et Cosmochimica Acta 73, 8: 2314-2331.

Kaszuba, J.P., Janecky, D.R., and Snow, M.G. (2003). Carbon dioxide reaction processes in a model brine aquifer at 200 degrees C and 200 bars: implications for geologic sequestration of carbon. Applied Geochemistry. 18, 7: 1065-1080.

Kneafsey, T.J. and Pruess, K. (2011). Laboratory experiments and numerical simulation studies of convectively enhanced carbon dioxide dissolution. Energy Procedia. 4: 5114-5121.

Kumar, A., Ozah, R. (2005). Reservoir simulation of CO_2 storage in deep saline aquifers, Society Petroleum Engineering.

Lin, H., Fujii, T. and Takisawa, R. (2008). Experimental evaluation of interactions in supercritical CO_2/water/rock minerals system under geologic CO_2 sequestration conditions. Journal of Materials Science 43, 7: 2307-15.

Lu, P., (2011). Navajo Sandstone-brine-CO2 interaction: implications for geological carbon sequestration. Environmental Earth Sciences. 62, 1: 101-118.

Luttge, A., Conrad, P., (2004). Direct Observation of Microbial Inhibition of Calcite Dissolution, Appl. Environ Microbial. 70, 3: 1627-1632.

Luquot, L. and Gouze, P. (2009). Experimental determination of porosity and permeability changes induced by injection of CO_2 into carbonate rocks. Chemical Geology. 265(1-2): p. 148-159.

Metz, B. (2005). IPCC special report on carbon dioxide capture and storage. Intergovernmental panel on climate change: 431.

Mohamed, R. S., Saldana, M. D. A. (2002). Extraction of caffeine, theobromine, and cocoa butter from Brazilian cocoa beans using supercritical CO_2 and ethane. Industrial & Engineering Chemistry Research 41(26): 6751-6758.

Oelkers E. H., Gislason S. R., Matter J. (2008) Mineral Carbonation of CO_2. Elements, 4 (5), 333-337.

Park, J., Sanford, R. A. (2009). Microbial activity and chemical weathering in the Middendorf aquifer, South Carolina. Chemical Geology 258(3-4): 232-241.

Raistrick, M., Mayer, B. (2006). Using chemical and isotopic data to quantify ionic trapping of injected carbon dioxide in oil field brines. Environmental Science & Technology 40(21): 6744-6749.

Rimmele, G. (2008). Heterogeneous porosity distribution in Portland cement exposed to CO_2-rich fluids. Cement and Concrete Research. 38(8-9): 1038-1048.

Roberts, J. A., Bennett, P. C. (2004). Microbial precipitation of dolomite in methanogenic groundwater. Geology 32(4): 277-280.

Rudge, J. F., Kelemen, P. B. (2010). A simple model of reaction-induced cracking applied to serpentinization and carbonation of peridotite. Earth & Planetary Science Letters 291(1-4): 215-227.

Shock, E.L., (2009). Minerals as Energy Sources for Microorganisms. Economic Geology. 104(8): 1235-1248.

Supercritical fluid. New World Encyclopedia, (2008), UTC. 4 Jul 2012, 23:44 <http://www.newworldencyclopedia.org/p/index.php?title=Supercritical_fluid&oldid=683499>.

Warren, L. A. (2001). Microbially Mediated Calcium Carbonate Precipitation: Implications for Interpreting Calcite Precipitation and for Solid-Phase Capture of Inorganic Contaminants. Geomicrobiology Journal 18, 1. 93-115.

Zhang W., Li Y. L., Xu T. F., (2009). Long-term variations of CO_2 trapped in different mechanisms in deep saline formations: A case study of the Songliao Basin, China International Journal of Greenhouse Gas Control. 3, 2, 161-180.

CHAPTER 2
GEOLOGIC SETTING

The western interior plains (WIP) aquifer system underlies most of Kansas, the eastern and southern parts of Nebraska, and a small area in west-central Missouri. In southern Kansas, the WIP system includes rocks of Ordovician and Cambrian age (Arbuckle Group), overlain by a shale unit of Mississippian to Devonian age (Chattanooga Shale), overlain by an oil producing Mississippian aged limestone, capped with a thick middle-Pennsylvanian aged shale unit (Cherokee Shale). The entire WIP aquifer system is being targeted for geologic carbon storage (GCS) in southern Kansas. The Arbuckle aquifer is the target reservoir for carbon sequestration and the Mississippian limestone targeted for enhanced oil recovery (EOR) (2010 Carbon Sequestration Atlas of the United States and Canada – Third Edition (Atlas III)).

Sanction of the Arbuckle aquifer system for GCS requires evidence of regionally significant seal integrity, substantiation of storage capacity estimates, and an assessment of probable plume behavior. This study attempted to address these needs by examining the integrity of the Chattanooga and Cherokee shales experimentally and by using baseline geochemical and microbiological data to explore the connectivity of the reservoir. The results have definite repercussions for caprock integrity, storage capacity and flow paths within the Arbuckle reservoir. We conclude that 1) Substantial reactivity will occur between CO_2 and the caprock materials but it is expected to be beneficial to seal capacity, 2) There is hydraulic separation between the Upper and Lower Arbuckle and 3). There is likely an extensive fracture network within the proposed injection zone of the lower Arbuckle. In order to model and predict injection behavior in the reservoir, it is important to examine the underlying geology, which dictates these conditions.

Study Area

Two wells, KGS 1-32 and KGS 1-28, were drilled from surface to granitic basement to examine the potential of the region for carbon sequestration and enhanced oil recovery within Wellington oilfield in Sumner County, Kansas (Fig. 2.1). Brine was sampled during four drill-stem-tests performed in each well. Coring began at a depth (below groundsurface) of 1079 m in KGS 1-32 and an almost continuous 500-meter long core was collected from the top of the Cherokee Shale to the granite basement. Three breaks in the core record were caused by extensive vugs and fractures in the reservoir that caused the core shaft to lock up. Conventional drilling was used to get through these zones before coring began again. Rock materials used in the experiments discussed in Chapters 4 and 5 were collected from this core. The two wells are located approximately 1065-meters apart (Fig. 2.1).

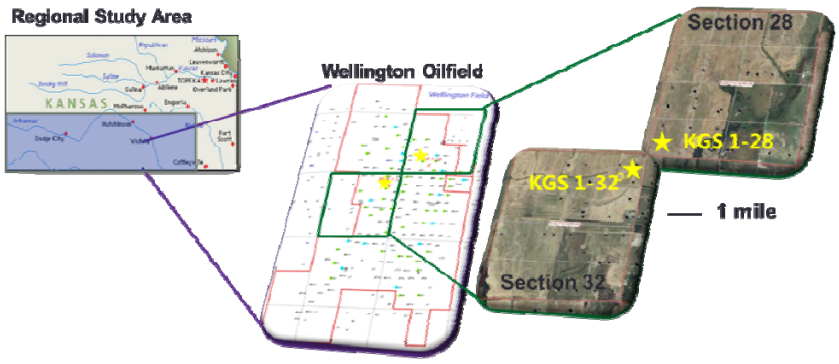

Figure 2.1: Study area map showing well locations from which brine and core materials were collected.

Stratigraphy

The stratigraphic succession of the 500-meter continuous KGS Core 1-32 collected in Wellington oilfield includes the 305-m thick stratigraphic succession from the Gunter Sandstone Member of the Gasconade Dolomite of the Arbuckle Group to the top of the Cherokee Shale. The span of geologic time covered by formations of interest in this study is Lower Ordovician to

the Middle Pennsylvanian. Table 1 and Figure 2.2 outline the stratigraphy and what purpose each rock formation serves in the CO_2 project.

Purpose	Stratigraphy	KGS 1-32 Top
Tertiary seal	Sumner Group Evaporites	185-365 m
Secondary seal	Cherokee Shale	1080 m
EOR reservoir	Upper Mississippian Series	1115 m
Alternate Primary seal	Lower Mississippian Series	1216 m
Primary seal	Chattanooga Shale	1239 m
Storage reservoir	Arbuckle Group	1239.1 m

Table 2.1. Table outlining the Stratigraphy and purpose of the Paleozoic rocks being examined for GCS applications in south-central Kansas and they role they would serve with their measured top depths in KGS 1-32.

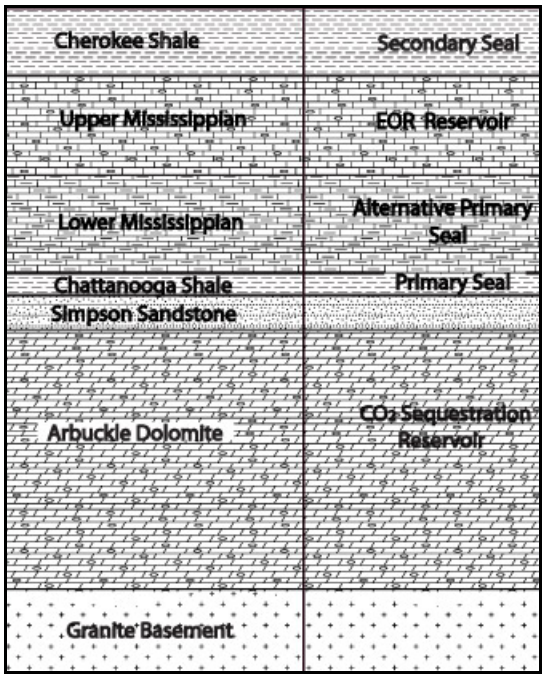

Figure 2.2. Stratigraphic column showing Paleozoic rocks being examined for GCS applications in south-central Kansas and they role they would serve.

Cherokee Group – EOR Primary-seal and Sequestration Secondary-seal

The Cherokee Group serves as a secondary-seal for carbon sequestration in the Arbuckle aquifer and as primary-seal for enhanced oil recovery purposes in the Upper Mississippian Series (Fig. 2.2). Within our study area, the Cherokee consists of all Pennsylvanian beds between the base of Fort Scott and the top of Mississippian limestone. Regionally, the group is made up of mostly shale, some sandstone, and sandy shale and occasional coal beds and a rare limestone. Up

to 18 formations have been recognized in the Cherokee Group, which can reach up to 152 meters in total thickness at outcrops in southeastern Kansas (Merriam, 1963). Partial recovery of the Cherokee Group observed in the 36 m of Cherokee Shale (1080 m-1115 m) captured in KGS Core 1-32 included a diverse range of lithologies, mostly paleosols, ranging from pale yellowish brown massive chert to dark greenish gray blocky mudstones. Well logs run in both wells indicate the presence of over 91 m of Cherokee shale in the study area. The Cherokee Shale, unlike the Chattanooga Shale, rarely thins to a thickness of less than 76 m in southern Kansas.

Mississippian Rocks

Mississippian age deposits in Kansas are primarily shallow-water carbonates. The maximum thickness of Mississippian rocks in the Hugoton embayment of southwestern Kansas is more than 515 meters (Franseen, 2004). Mississippian rocks in Kansas are subdivided into the Upper Mississippian Series and the Lower Mississippian Series.

Upper Mississippian Series – Enhanced Oil Recovery

The Upper Mississippian Series in Kansas consists predominately of beds of limestone and dolomite with interspersed beds of sandstone and shale and minor amounts of chert (Zeller, 1968). The series is comprised of the Meramecian Stage overlain by the Chesterian Stage. The Chesteran Stage is separated from the Pennsylvanian rocks above by an unconformity. This series contains the oil-producing units of Wellington oilfield and is currently the target of secondary enhanced oil recovery via CO_2-flooding within Wellington oilfield (Fig. 2.2). Wellington oilfield has been water flooded in the past and to date has produced over 3-billion liters of oil (http://www.kgs.ku.edu/Magellan/Field/index.html). KGS Core 1-32 collected 70.9 m (1115 m-1186 m) of the Upper Mississippian Series. The Upper Mississippian Series is distinguishable from the Lower Mississippian Series by an increase in carbonate and a decrease

in argillaceous material. The lithology of the Upper Mississippian Series ranges from a dark gray moderately argillaceous fine peloidal limestone to an olive gray bioturbated micritic lime mudstone interbedded with pale yellowish brown massive chert.

Lower Mississippian Series – Potential Alternate Primary-seal

The Lower Mississippian Series in Kansas consists of beds of shale, limestone, dolomite and chert with cherty dolomite dominating the sequence. The series is composed of the Kinderhookian Stage overlain by the Osagian stage (Zeller, 1968). Approximately 52.5 meters of the Lower Mississippi Series (1186 m-1238.5 m) was present in KGS Core 1-32. This series is of particular interest because of the tight and uniform nature of the rocks indicates it may be suitable as a widespread regional seal for the Arbuckle aquifer (Fig. 2.2). Core measurements show porosities of these rocks ranges from 0.58% to 7.16% and permeabilities as low as 4.93×10^{14} m^2. The zone from 1211.5 m-1229 m is especially prominent as a potential seal. The rocks in this zone are tight, very dark greenish gray to medium dark gray argillaceous dolomitic siltstones.

Chattanooga – Primary-seal

The Chattanooga Shale is Upper Devonian to Lower Mississippian in age and is considered the primary seal for CO_2 sequestration in the region (Fig. 2.2). The Chattanooga Shale is dolomitic, silty, and often pyritiferous. Its thickness is variable in southern Kansas and ranges from 1 to 50 meters and is separated from underlying rocks by an angular unconformity. It is notably absent at the north end of the Nemaha anticline (Zeller, 1968). Thickness of the Chattanooga varies considerably across the region (Fig. 2.3). Data collected between KGS 1-28 and KGS 1-32 highlight this variation. Well logs ran in KGS 1-28 indicated approximately a 15-

meter thick section of Chattanooga Shale. However, KGS 1-32, drilled just 1065 meters away from KGS 1-28, had only a 15-centimeter thick section of Chattanooga Shale.

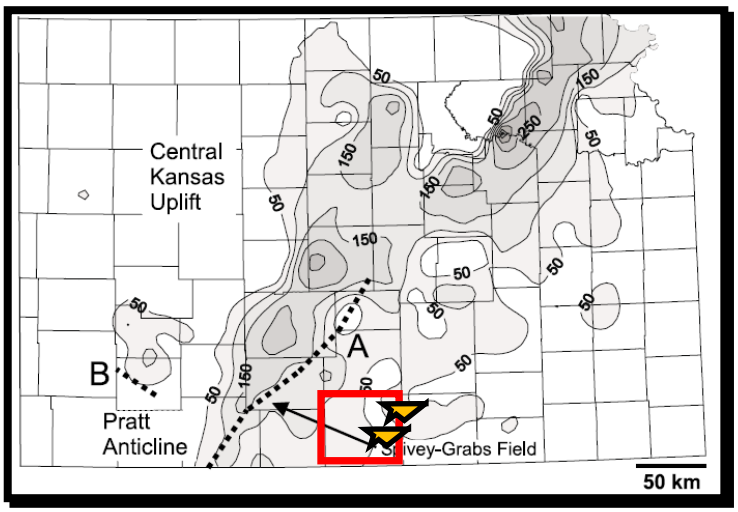

Figure 2.3: Isopach of showing thining of the Late Devonian- Early Mississippian Chattanooga Shale & Kinderhook Shale around Wellington oil field.

Simpson Group - CO_2 storage reservoir

The Simpson Group includes several sandstones and limestones (Zeller, 1968). Although the Simpson Group can exceed 450 meters in areas of Oklahoma, it has been almost entirely eroded away across Kansas and typically is no more than 30 meters thick. The Simpson Group lies between the storage reservoir and the primary seal and is considered as part of the carbon storage reservoir.

Arbuckle Group – CO_2 storage reservoir

KGS Core 1-32 reached the top of the Arbuckle at 1270 m and retrieved 305 m of the Arbuckle Group (1270 m-1574 m). The Arbuckle Group thickens to the southeast, into Oklahoma and Missouri (Zeller, 1968). The Arbuckle is often used as a disposal reservoir although the formation is typically only shallowly penetrated. In contrast, the injection of CO_2 would occur at the base of the formation and attempt to take advantage of the storage capacity of the entire Arbuckle Group. This study examines the connectivity of the reservoir, which is

expected to be largely dictated by the different facies of the three formations encountered in this section of the Arbuckle Group. For that reason, descriptions of the undifferentiated Jefferson City-Cotter dolomites (JCC), Roubidoux, and undifferentiated Gasconade dolomite-Gunter sandstone are presented here starting at the top of the Group. Core 1-32 showed that the Eminence dolomite is not present in the study area, therefore it is not described herein.

Jefferson City-Cotter dolomite (JCC)

The rocks of the Jefferson City-Cotter dolomite (JCC) were described by Zeller (1968) as consisting mainly of coarsely granular, cherty dolomite with the upper part of the unit being oolitic chert transitioning to tripolitic chert towards the base of the unit. Preliminary description of KGS 1-32 indicate the JCC in nearly 148 meters-thick (Top at 1269.7 m) in Wellington oil field with the upper part of the unit being medium-grained packstone to grainstones interbedded with argillaceous dolomite and the lower portion being dominantly composed of micritic dolomite (Personal communications with Lynn Watney and Paul Gerlach). Correlations between the core and 3D-seismic acquired for the project show the lower JCC corresponds to a high impedance zone indicating tight, dense rock. Chapter 3 discusses the impact this tight unit has on the hydraulic connectivity of the reservoir.

Roubidoux

The rocks of the Roubidoux Formations were described by Zeller (1968) as mainly sandy dolomite and fine-grained sandstone and ranges in thickness between 45-60 m. The Roubidoux, however, is 79 m-thick in KGS 1-32 (Top at 1416.8 m). Several sections of the formation could not be recovered by coring operations; 1419.1 m to1426.5 m and 1468.7 m to 1493.5 m. Magnetic Resonance logs indicated the presence of large vugs and fractures in each of these zones, which likely caused the lack of recovery. Chapter 3 of this study discusses the

geochemical evidence for connectivity between the Roubidoux and Gasconade formations due to extensive fracturing in lower portion of this formation.

Gasconade dolomite

The rocks of the Gasconade were described by Zeller (1968) as a cherty, coarsely granular dolomite ranging in thickness from 0-61 meters with a prominent sandy dolomite member known as the Gunter sandstone. The Gasconade is 76.7 m-thick in KGS 1-32 (Top at 1496 m) and rests unconformably on the Pre-Cambrian basement at 1573 m-depth. A section of the formation could not be recovered by coring operations; 1523.3 m to1539.1 m. Magnetic Resonance logs indicated the presence of large vugs and fractures in this zone, which likely caused the lack of recovery. CO_2 injection will take place in the base of the Gasconade formation. Chapter 3 of this study discusses the geochemical evidence for extensive fracturing in lower portion of this formation as well.

References

Department of Energy (2010). Carbon Sequestration Atlas of the United States and Canada – (Atlas III) (Third Edition): 159.

Merriam, D. (1963). The Geologic History of Kansas. Kansas Geological Survey Bulletin: 317.

http://www.kgs.ku.edu/Magellan/Field/index.html Kansas Geological Survey Production from Kansas Oil and Gas Fields. Accessed 2/7/2012.

Watney, L. W., (2011). KGS 1-32 core description.

Zeller, D. (1968). The stratigraphic succession in Kansas. State Geological Survey of Kansas. Bulletin 189: 76.

CHAPTER 3

Geochemical, Microbiological, and Permeability Characteristics Indicating Vertical Zonation of the Arbuckle Saline Aquifer, a potential CO_2 storage reservoir

ABSTRACT

The Kansas Geological Survey (KGS) is evaluating the western interior plains (WIP) aquifer for its potential for carbon sequestration and enhanced oil recovery. In this study we explore the extent and relevance of heterogeneity of the lower WIP, composed primarily of the Arbuckle Group, to the application of carbon storage. Using geochemical, petrophysical, and microbiological characterization of two 1600 m long boreholes and a 500 m long core collected from one of these wells located within Wellington oil field, located in Sumner County, Kansas, we present evidence of the presence of a significant central baffle in the reservoir and assess the extent of the hydraulic separation between the Upper and Lower Arbuckle.

INTRODUCTION

Geologic carbon storage (GCS) has gained recognition as a feasible method for disposing anthropogenic CO_2 underground and reducing atmospheric CO_2 concentrations. CO_2 can be successfully sequestered for hundreds to millions of years in geological formations by pore space trapping of CO_2 gas, dissolution into brine water, and by in-situ precipitation through mineral carbonation (Gunter et al., 2000). Spent petroleum reservoirs and deep saline aquifers are targeted for these activities due to their storage capacity, depth and isolation from the surface and extensive geographic distribution (e.g. Bachu, 2002). The Arbuckle Group in Kansas was identified by Carr et al. (2005) as a prodigious storage reservoir for CO_2 because it exhibits many of the ideal CO_2 storage qualities including a large storage capacity, porous carbonate and

sandstone rocks, and highly saline waters. Each GCS site is geologically unique which calls for detailed geochemical, structural, stratigraphic, and biogeochemical characterization to assess its efficacy for CO_2 storage.

Several sites have injected CO_2 into subsurface formations (Kharaka et al.,2006 and 2009; Emberley et al., 2005; Romanak et al., 2012; and others) and field studies have been crucial for validating findings from simplified and controlled laboratory experimentation (Kaszuba, 2005; Luquot and Gouze, 2009; Zemke et al.,2010; Carroll et al., 2011; and others). Kharaka et al. (2009) found that CO_2 injection into a sandstone unit of the Frio Formation caused a decrease in pH, an increase in alkalinity, and increase in dissolved iron in the system possibly due to corrosion of pipe and well casings. Recent work has acknowledged that perturbation of subsurface microbial communities during CO_2 injection may impact seal integrity or pipe corrosion because microorganisms are intimately linked to solution geochemistry. While some have speculated that many deep aquifers targeted for CO_2 storage lack nutrients and energy sources to support microbial life, studies over the past three decades strongly suggest the contrary is true (Amy and Halderman, 1997; Magot et al., 2000; Pedersen, 2000).

Recent work by Morozova et al. (2010; 2011) and Wandrey et al. (2011) reported that microorganisms were present in concentrations ~10^6 cells ml^{-1} in a deep saline aquifer in Ketzin, Germany, and were able to survive and adapt to supercritical CO_2 ($CO_{2(SC)}$) exposure. Native microorganisms can actively alter mineral equilibria (Ehrlich, 1996; Welch et al, 1994e) through metabolic activity, pH, concentration of elements, alteration of organic compounds (Shock, 2009) and the ability to harvest energy from numerous oxidation and reduction reactions (Croal et al., 2004). Because microbial metabolic activity could affect the potential for carbon sequestration in the Arbuckle reservoir we included characterization of native microbial

consortia and geochemistry in our assessment of reservoir connectivity and isolation from overlying units.

Geological investigations of the Arbuckle Group by Franseen et al., (2004), Carr et al. (1986) and others have demonstrated that the Arbuckle Group is both laterally and vertically heterogeneous. In this study we explore the extent and relevance of that heterogeneity to the application of carbon storage, through planned SC-CO_2 injection into the high-permeability zone near the base of the Arbuckle aquifer in Kansas. Using geochemical, petrophyscial, and microbiological characterization of two 1600 m long boreholes and a 500 m long core collected from one of these wells located within Wellington oil field, located in Sumner County, Kansas, we present evidence for flow baffles created by discontinuous aquitards and assess the extent of isolation by regional and local confining units.

EXPERIMENTAL SECTION

Two 2.15 km-deep wells, KGS 1-32 and KGS 1-28 (injector), located within the Wellington oil field in Sumner County, Kansas were drilled in January and June 2011. The two wells are located approximately 1050-meters apart. KGS 1-32, 500-meter long core, captured the entire geologic section between the Cherokee Shale and Pre-Cambrian granite, including the 305-meter thick section of the Arbuckle dolomite, (Fig. 3.1). Core was collected in 18.3-meter sections using a CT510 Core Bit with a conventional split ring core catcher using two 9.15-meter joints of aluminum casing that was cut into 1-meter segments, and stacked on pallets for transport to the Weatherford Labs facility in Houston, Texas.

Drill stem fluids were obtained from intervals in KGS 1-32 with averaged depths of: 1121 m, 1277 m, 1321 m, 1378 m, 1502 m, 1535 m, and 1582 m. The test from 1121 m was run in the oil producing Mississippian formation, which lies directly above the Arbuckle and the test

from 1582 m is in the underlying granite basement. The intervals from 1121 to 1582 m were run in the Ordovician-aged Arbuckle Group, which includes the Gunter sandstone, Gasconade dolomite, Roubidoux formation, and the Jefferson City-Cotter (JCC) dolomite at the top of the group, which is the targeted location for a 40,000 tonne CO_2 injection. The Simpson sandstone is bounds the Arbuckle above is also part of the storage reservoir. Additionally, four depths were perforated in the completed borehole KGS 1-28 for sampling, with average depths for each interval, 1332 m, 1486 m, 1502 m, and 1527 m.

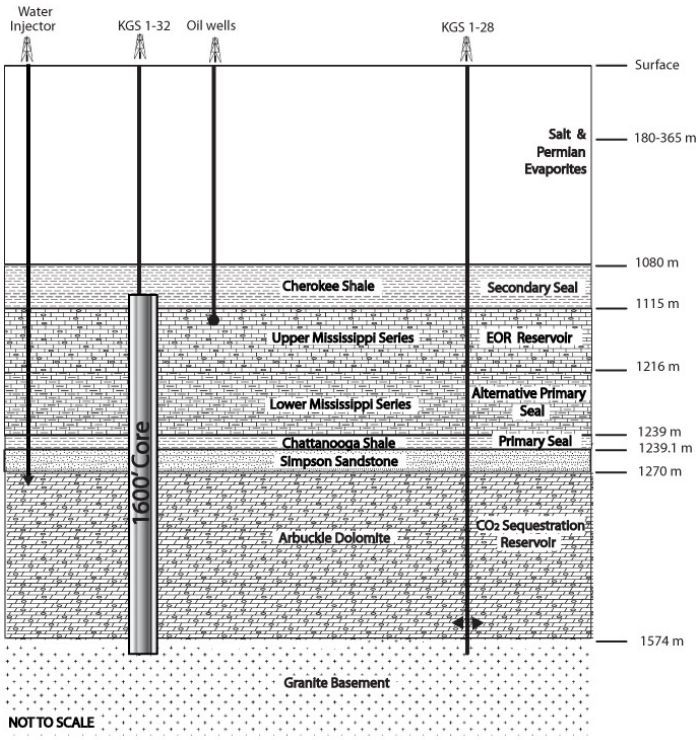

Figure 3.1. Generalized cross-sectional schematic showing the relevant stratigraphic units for CO_2 storage and CO_2 enhance oil recovery and corresponding seals with approximate well penetration depths of KGS 1-32, KGS 1-28, existing Mississippian production wells and Arbuckle disposal wells, as well as the cored interval of KGS 1-32 at the Wellington oil field in Sumner County, Kansas. Depths are in meters. Not to scale.

Field methods

Physical and Chemical Rock Characterization

Reservoir characterization was accomplished using an extensive suite of wireline logging tools run through the borehole after completion. Geochemical logs were collected to detect

changes in mineral abundances using variability in bulk chemical composition. Continuous chemical analyses were obtained using Halliburton's GEM Elemental Analysis Tool, which is a neutron-induced capture gamma ray spectroscopy logging system designed to derive elemental contributions contained within the total measured gamma ray energy spectrum (www.**halliburton**.com/publicL[-1]p/contents/Data.../H06648-A4.pdf). The output of energy spectra are converted to dry weight percent concentrations of aluminum, calcium, iron, potassium, magnesium, silicon, sulfur, titanium and manganese.

Nuclear magnetic resonance (MRI) provides information on pore size distribution and permeability indicators. The Timur-Coates transform (Delhomme, 2006) was used to determine the permeabilities used in this study (Fig. 3.2). The variation in permeability is an expression of variability in grain-size, pore-size, pore-throat size, and degree of cementation that varies throughout the 305-meter thick Arbuckle dolomite.

After the core was examined and described in detail, 17 samples were collected for elemental carbon, nitrogen, and phosphorus analyses. Samples were selected from within the same zones as the brine samples were collected during drill-stem tests (DSTs) and swabbing intervals where possible. One half gram of each sample was analyzed for total carbon and nitrogen on a LECO CN 2000 combustion analyzer which reports total levels (inorganic and organic) of C and N on a weight percent basis. One gram of each sample was also analyzed for total nitrogen and phosphorus using a flow elemental analyzer after a modified-Kjeldahl digestion.

Chemical and Microbiological Solution Characterization

Drill stem tests purged varying volumes of water from 160 to 6400 liters, which included drilling mud, depending on recovery. Samples were collected from the final 20 liters, containing

the least drilling materials. Perforation of the completed boreholes flushed ~5000 liters of water, of which the final 20 liters was sampled. As the perforation tests contained no drilling mud they were used to assess major contributions to DST samples by mud as well as comparisons for the impact of borehole drilling on aquifer biogeochemistry. Test depths were selected using well log data to assure characterization of both the high porosity and low porosity zones in the Arbuckle aquifer and to allow for suitable coverage for elemental depth profiles and microbial characterization.

pH was measured up-hole immediately after collection using a portable pH meter and electrode. Temperature was measured on the DST down-hole tool. All water samples, except headspace gas, were filtered in the field using 142 mm diameter Whatman glass fiber prefilters and a 0.45um Millipore PVDF membrane filter and held at 4 C until analysis. Samples for stable isotopic analysis of DIC were purged with helium gas for five minutes and acidified with 1.5 ml of phosphoric acid and analyzed with a Thermal Electron Gas Bench coupled to a Thermal MAT 253 Mass Spectrometer (MS). Cation analyses were performed using Inductively Coupled Plasma Optical-Emission Spectroscopy (ICP-OES; Perkin Elmer Optima 5300DV) on a filtered sample acifidied in the field to 2% Nitric Acid (Fisher Scientific, Certified ACS Optima). Anions were measured on a filtered sample using an Ion Chromatography (IC; Dionex ICS 3000, Thermo Scientific). Alkalinity was determined using a 0.2-μm filtered, un-acidified sample by a manual titration to pH = 3 and endpoint determination, within 48 hours of collection. Fixed gases were quantified from headspace of raw water injected into sealed serum bottles preserved with mercuric chloride using a gas chromatography (GC; Agilent Technologies 6890N) fitted with a flame ionization detector (FID). $\delta^{18}O_{CO2}$ and δD of 1.5 ml of filtered brine were analyzed using a Picarro Cavity Ring-Down Spectrometer.

Molecular and culturing methods were used to confirm the presence of and characterize the microbial community. The Most Probable Number (MPN) technique was used in an effort to culture and characterize the microbial physiology of native microorganisms. We targeted fermenters, dissimilatory iron reducing bacteria (DIRB), sulfate reducing bacteria (SRB) and methanogens based on the anoxic nature of the aquifer. Media formulations are included in Appendix Table C.1-C.4. All media contained 8% salinity (as NaCl) to match the average salinity of the Arbuckle saline aquifer. After inoculation with raw water in the field, bottles were over-pressured with 70% H_2/30% CO_2 and incubated at 50ºC in the dark. Fermenters were scored for growth, on the basis of media clarity, after two weeks. DIRB were scored using the presence of Fe(II) compared to controls after eight weeks. SRB were scored using the presence of sulfide, compared to controls, on lead acetate paper after eight weeks. Methanogens were scored by measuring headspace methane concentrations compared to controls after eight weeks. MPN for each physiologic type were calculated using the MPN Calculator (shareware maintained by John Lindquist at the University of Wisconsin, http://www.abbrv.co.uk/j93).

DNA was extracted from 142-mm diameter filters that had 3 L of formation water filtered through by first suspending the filter in TE-sucrose buffer, then treating with lysozyme, sodium dodecyl sulfate (SDS), and proteinase K. After incubation at 37 ˚C, Bio101 beads were beaten for 30 sec. Extraction with a 1.2:1 ratio of 5M NaCl and 10%CTAB followed with incubation at 65 ˚C. DNA was purified with 24:1 chloroform:isoamyl alcohol and 25:24:1 phenol:chloroform:isoamyl alcohol. The DNA was precipitated with isopropanol and washed with 70% ethanol. After resuspending the DNA in water, samples were incubated overnight at 4 ˚C and stored in a -20 ˚C freezer until further analysis.

The bacteria and archaea 16s rRNA gene fragments were amplified using primers listed in Appendix Table A.2. Each primer set was run in a PCR mixture of 20 µl containing Qiagen Q-solution, 10x buffer, MgCl, and BSA along with the DNA template. The thermocycler was run with a taq initiation step at 95 ˚C for 3 min, followed by 30 cycles of a denaturing step of 94 ˚C for 1 min, an annealing step at 47 ˚C for 45 sec, and an elongation step at 72 ˚C for 45 sec. After the 30 cycles, a final extension occurred at 72 ˚C for 7 min. No detectable archaeal DNA was amplified during the procedure. The PCR products of the two bacterial primer sets were mixed, and cloning followed using the Invitrogen TOPO TA cloning kit. Final cloning products were sent to Functional Biosciences (Madison, WI) for sequencing. Sequences were trimmed using FinchTV, and chimeras were detected using Bellophon (Huber, 2004). Sequences with 97% similarity were grouped into OTU's on the genus level using Mothur and NCBI Blast (Altschul, 1990, Schloss, 2009). In cases where OTU's were less than 97% similar to a family, the microorganisms were not included in the ecological figures or discussion.

DNA was quantified by qPCR procedures, using primers listed in Appendix Table A.2. The primer set and probe was run in a PCR mixture with a total volume of 20 µl containing Applied Biosystems TaqMan Master mix along with the DNA template. The thermocycler was run with an initiation step at 50 ˚C for 2 min and denaturing of 95 ˚C for 10 min, followed by 40 cycles of 95 ˚C for 15 sec and 56 ˚C for 1 min. Diluted samples of known concentrations of *E. coli* were used as standards, where the *E. coli* was quantified with Quant-iT™ PicoGreen ® dsDNA Reagent and Kits procedures.

RESULTS AND DISCUSSION

Reservoir Characterization. The cored section of Arbuckle dolomite is over 300-meters thick (1269 m - 1574 m below ground surface) and exhibits diverse lithologies ranging

from; very porous medium pelleted dolomitic packstones and coarse grainstones (1335 m), tightly cemented peloidal dolomitic packstones with no porosity, vugs or fractures (1381 m), dense micritic dolomite (1415 m), dolomitic breccias with discontinuous solution enhanced fractures (1445 m), and micritic dolomitic mudstones with mm-sized pyrite clusters and fossil fragments (1465 m). Fractures are common but are characteristically vertical, short, unconnected and bedding constrained. The heterogeneity of the reservoir caused by varied depositional facies and the resulting variable permeabilities associated with these facies observed in the wells logs (Franseen, 2004) could encourage the desired hampering of the path of otherwise buoyant CO_2, accelerate pore space trapping and dissolution (Kneafsey and Pruess, 2011). Kneafsey and Pruess used laboratory visualization studies to investigate these effects.

Examination of the cored section of KGS 1-32 showed the Arbuckle saline aquifer is mostly cherty dolomite [(SiO_2) and ($CaMgCO_3$)]. This validated the results from geochemical logs, which indicated calcium, magnesium and silica were present in the highest elemental abundances of all the elements evaluated (Al, Ca, Fe, K, Mg, Si, S, and Ti). On average, calcium comprised 20.1% of the rock by weight percent, magnesium 8.1% and silicon 7.5%. In chert-rich zones, silica is much higher and makes up to 43.4% of the rock by weight percent. Aluminum, iron, potassium and sulfur are lower in concentration and fluctuate slightly throughout the reservoir. Aluminum varies between 0 to 5.3%, iron from 0 to 1.2%, potassium from 0.6 to 2.2% and sulfur from 0 to 2.7%. The elemental abundance of aluminum was used to identify location and relative quantities of clay minerals based on the work by Herron and Herron (1998), which showed elemental abundances can serve as rapid but accurate lithologic indicators and provide a more accurate estimation of clay mineral content than gamma ray logs (Fig. 3.2).

Similar to the reservoir rocks, calcium and magnesium were also present in high concentrations in the aqueous phase, averaging 209 and 68 mmol L^{-1} respectively. Silicon averaged 0.3 mmol L^{-1} in the aqueous phase through the reservoir, which values calculated using PhreeqC indicated was under-saturated with respect to amorphous silica (Figure 4.4 and Appendix Tables D.2 and D.3). Aluminum is present is similar concentrations as silicon and follows the same trend. Calcium and magnesium are present in high concentrations in the aqueous phase and PhreeqC indicated the brine was oversaturated in regards to dolomite at all depths except 1527 m. The brine was oversaturated with aragonite and calcite throughout most of the reservoir but became slightly undersaturated towards the base of the reservoir (Figure 4.4 and Appendix Table D.2). The aqueous concentrations of calcium, magnesium and silicon with the geochemical log data highlighting these relationships. In addition to calcium and magnesium, the reservoir fluids have high concentrations of chloride, sodium, and potassium, which are expected from accumulation of salts in the reservoir over time (Dickey, 1966). Ion concentrations of swabbed brine show that the presence of drilling mud in samples collected during DSTs had no (within error) impact on geochemical analyses.

The aqueous concentrations of Ca^{2+}, Mg^{2+}, Si^{4+}, Na^{1+} and K^{1+} increase with depth within the Arbuckle aquifer linearly with R^2 values of 0.9 or higher. It is characteristic for ion concentrations in oilfield brines to increase with depth (Dickey, 1966). This linearity of the data suggests there is connectivity at some timescale throughout the reservoir. This could be indicative of several degrees of connectivity on various timescales; 1) the entire 305-meter thick reservoir could be isotropically permeable with mixing via diffusion over hundreds to thousands of years, 2) the reservoir could be anisotropically permeable but not so much so that diffusion

does not occur over those long time scales, 3) fractures in the reservoir might be providing hydraulic communication and mixing on a much shorter timescale.

Permeability values derived from NMR wireline logs highlight the heterogeneity within the Arbuckle Group formations which include the Gunter sandstone, Gasconade dolomite, Roubidoux formation, and the Jefferson City-Cotter dolomite at the top of the group. The log calculated permeabilities range from $3.10x10^{-13}$ m^2 to as low as $2.07x10^{-18}$ m^2. In comparison, permeability (Kmax) measurements of KGS 1-32 core samples range from $1.97x10^{-16}$ m^2 to $1.28x10^{-12}$ m^2. Permeability values calculated from the NMR wireline logs are typically biased with matrix compared to direct core measurements when data from the same location is compared. Permeability estimates were also calculated for each of the drill-stem tested zones using Horner plots. Thickness of the zone with 8% or greater porosity was used and resulted in permeability estimates of $1.97x10^{-16}$ m^2 at 1277 m, $1.13x10^{-14}$ m^2 at 1321 m, $2.55x10^{-12}$ m^2 at 1378 m, $9.87x10^{-14}$ m^2 at 1502 m, $1.09\ x10^{-13}$ m^2 at 1535 m, and $7.90\ x10^{-16}$ m^2 in the granite basement at 1582 m. The highest Timur-Coates permeabilities coincide with gaps in the core recovery because core jamming occurred when there was pervasive fracturing or vuggy sections.

Because the log values provide information over the entire reservoir, calculated permeability estimates using the Timur-Coates transform are plotted with elemental abundance of Al^{3+} in Figure 3.2 to show the absence of a correlation between increased clay content and decreased permeability. These data suggests that clay mineral content is not the source of variation in permeability in the reservoir. Permeability values are particularly low between 1332 m^{-1}460 m (Fig. 3.2), qualifying it as a potential baffle which coincides with the lower JeffersonCity-Cotter formation, a tight, dense, micritic dolomite. Seismic data collected within the study area also reported high seismic impedance for the middle Arbuckle (1339 m^{-1} 461 m)

indicating high density rocks which largely overlaps the zone of low permeability observed in the well logs. Core description from this 122-meter zone identified lithologies ranging from micritic dolomite, dolomitic mudstone, shaley dolomite, to peloidal packstones with occassional thin (~0.3 to 1.0 m) zones of breccia and chert with micritic dolomite by far being the dominant lithology over the interval. The micritic dolomite observed in core was typically tight, dense, with a lack of substantial porosity although occassional inter-crystalline porosity was noted. The minor minerals of the Arbuckle reported have included calcite ($CaCO_3$), pyrite (FeS_2), kaolinite ($Al_2Si_2O_5(OH)_4$), illite ($(K,H_3O)(Al,Mg,Fe)_2(Si,Al)_4O_{10}[(OH)_2,(H_2O)]$), siderite ($FeCO_3$), and anhydrite ($CaSO_4$) (Zeller, 1968).

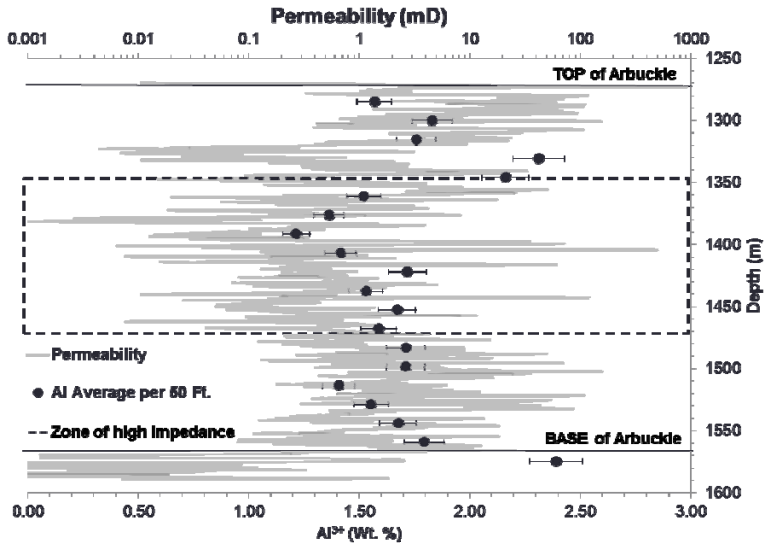

Figure 3.2. Permeability and clay content of suspected baffle unit. Permeability measurements displaying a decrease in overall permeability throughout the middle Arbuckle Group and weight % concentrations of Al^{3+} as an indicator for clay concentration (Herron, M.M., and Herron, S.L., 1998) in the reservoir rock averaged in fifteen meter intervals to show the lack of correlation between increased clay content and decreased permeability. The zone with low permeability corresponds to an interval of high impedance (dotted line) observed in seismic data indicating high density rock.

The temperature range of the Arbuckle in KGS 1-32 ranged from 43.9°C near the top of the Jefferson City-Cotter (JCC) formation (1277 m) to 54.4°C near the base of the Eminence dolomite (1535 m). The final shut-in pressures from DSTs in KGS 1-28 and KGS 1-32 indicates the pore pressure of the reservoir ranges from 1.18 $x10^{+7}$ Pascals (Pa) at the top of the JCC to

1.47 x10^{+7} Pa near the base of the Eminence dolomite. Geochemists Workbench was used to calculate pH under reservoir conditions under the assumption of brine saturation with dolomite, which confirmed that the pH is lower in the subsurface than measured at the surface; modeled pHs of 6.27 at the top of the Arbuckle (1277 m) grading to 5.69 (1535 m). A steep salinity gradient was observed in KGS 1-32 and KGS 1-28. Chloride values were measured at 969 mmol L^{-1} (3.4% salt) at the top of the reservoir (1277 m) and increase linearly (R^2 = 0.97) to 3114 mmol L^{-1} (11.0 % salt) at the base of the reservoir (1535 m).

Biogeochemical Indicators. Concentrations of redox reactive ions; ferrous iron, sulfate, nitrate and phosphate (Fe^{2+}, SO_4^{2-}, CH_4, NO_3^-) present in the reservoir fluids do not follow the same trends with depth as the major ions (Fig. 3.3). These ions are often used as evidence of biological activity in the subsurface (Beveridge, 1989). Geochemical logs show that on average, sulfur only makes up 0.63% of the reservoir rocks by weight percent, iron 0.34%. The concentration of ferrous iron increased sharply, from 0.5 to 3.0 mmol L^{-1} between 1321 m and 1378 m depth and then decreased to 2.1 mmol L^{-1} between 1378 m and 1502 m depth but remained stable around 2.1 mmol L^{-1} to a depth of 1535 m. Higher concentrations of reduced iron, 6.3 mmol L^{-1}, were measured within the granite basement rocks at a depth of 1582 m. Although sulfur is present in low abundance in the rocks, sulfate (SO_4^{2-}) is found in high concentrations in the Upper Arbuckle, 8.4 to 15.3 mmol L^{-1} between 1277 m to 1321 m and then steadily decreased to 2.8 mmol L^{-1} between 1321 m and 1535 m signifying the reduction of sulfate to sulfide. Some evaporite structures are preserved in the rock but have been replaced by silicification so no gypsum remains. Sulfate-reducing bacteria (SRB) acquire energy through oxidation of organic carbon or molecular hydrogen while reducing sulfate to hydrogen sulfide. Dissolved organic carbon available to SRBs in the Arbuckle range from 1 to 19 mmol L^{-1}

(Appendix Table D.1). Potential evidence of microbial methanogensis is also present. Methane concentrations were measured at 0.7 mmol L^{-1} at 1277 m and 1321 m and then drew down sharply to 0.06 mmol L^{-1} at 1378 m (Fig. 3.4). Methane concentrations then began to increase again with depth reaching a concentration on 0.09 mmol L^{-1} at 1535 m, which could be indicative of methanogenesis. δC^{13} become enriched with depth. δC^{13} at the top of the reservoir are -24.4 $^{o}/_{oo}$VPDB and increase to -9.5 $^{o}/_{oo}$VPDB in the granite basement. These values are not as fractionated as is expected for methanogenic fractionation of carbon (Whiticar, 1999), but is still a possbility. Typical stratification of microbial metabolisms is DIRB above SRB above methanogens, indicated by a zone with increased reduced iron over decreasing sulfate (or increasing sulfide) over increasing methane. However, there appears to be two separate trends observed in the Arbuckle aquifer; one trend for the samples above the suspected baffle (1277 m to 1321 m), and one trend below the suspected baffle (1378 m to 1582 m) (Fig. 3.3). This suggests of reset of the biogeochemistry due to lack of hydraulic communication between the Upper and Lower Arbuckle.

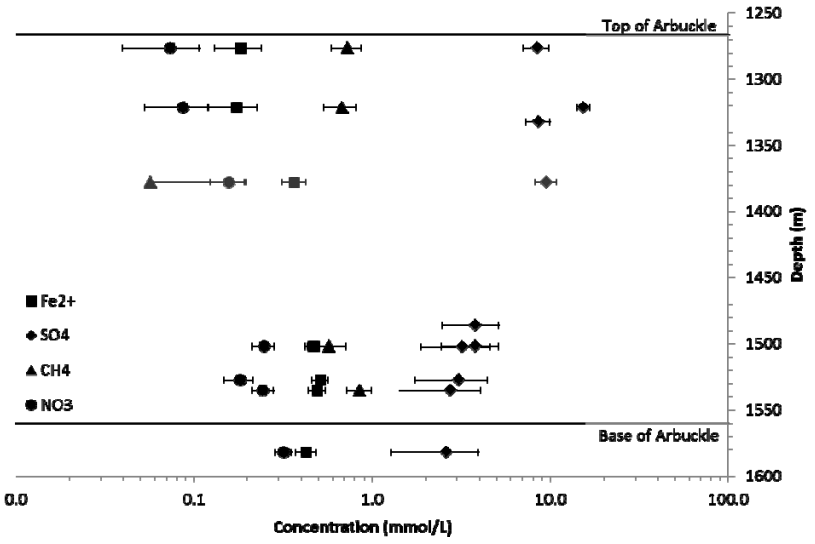

Figure 3.3. Concentrations of redox reactive ions; ferrous iron, sulfate,methane, and nitrate (Fe^{2+}, SO_4^{2-}, CH_4, NO_3^-) present in the reservoir. Typical stratification of microbial metabolisms is DIRB above SRB above methanogens, indicated by a zone with increased reduced iron over decreasing sulfate over increasing methane. However, there

appears to be two separate trends within the Arbuckle aquifer; one trend for the samples above the suspected baffle (1277 m to 1321 m), and one trend below the suspected baffle (1378 m to 1582 m). This suggests of reset of the biogeochemistry due to lack of hydraulic communication between the Upper and Lower Arbuckle.

Nutrient Availability. In addition to TEAs, microorganisms require nutrients to be active. Carbon, nitrogen, and phosphorous are typically the major biolimiting nutrients of oligotrophic environments like the deep subsurface (Wang et al., 1996). The depth (>1250 m) of the reservoir, the distance from outcrop recharge (~200 miles) and low flow rates estimated between 0.018 to 0.70 m^{-1} year (Birdie, T., verbal communication), and very high chloride values point toward minimal freshwater recharge of the Arbuckle in these region. Consequently, the best source of nutrients may be the reservoir rocks themselves (e.g., Rogers and Bennett, 2004). C, N, and P elemental analyses were performed on rock, while carbon, as dissolved organic carbon (DOC), nitrogen, as nitrate, and phosphorus, as phosphate concentrations were also measured in the brine. Average elemental analyses of 18 samples collected from core throughout the Arbuckle Group show the C:P in the rock was 18,600:1 which is more than an order of magnitude larger than the C:N at 1300:1 reflecting the lower concentration of phosphorus than nitrogen in the rocks. This gave an average C:N:P ratio of 16,000:12:1 for the reservoir rocks. The averaged relative nutrient concentrations in the brine are similar to those in the rocks with an average C:N:P ratio of 51,000:11:1. Each organism has a unique atomic ratio of carbon, nitrogen and phosphorus but the Redfield ratio (C:N:P – 106:16:1) is commonly used to assess the nutrient limitations of marine organisms and similar ratios (186:13:1) have been observed for soil biomass and (60:7:1) within soil (Cleveland, 2007). The C:N ratios in the Arbuckle range from over 15,000 to 361 and the C:P ratios range from 3249 to over 138,000 indicating the system is not carbon limited, but rather significantly N and P limited. Despite nutrient limitation biomass concentrations of 2.1 $x10^{6}$, 1.9 x 10^{7} and 2.6 x 10^{-3} cells ml^{-1} were determined using qPCR procedures. The lowest biomass coincides with the low permeability and high impedance

zone of the lower JCC formation. Decreased flow through this low permeability zone could decrease nutrient recharge and lead to nutrient depletion.

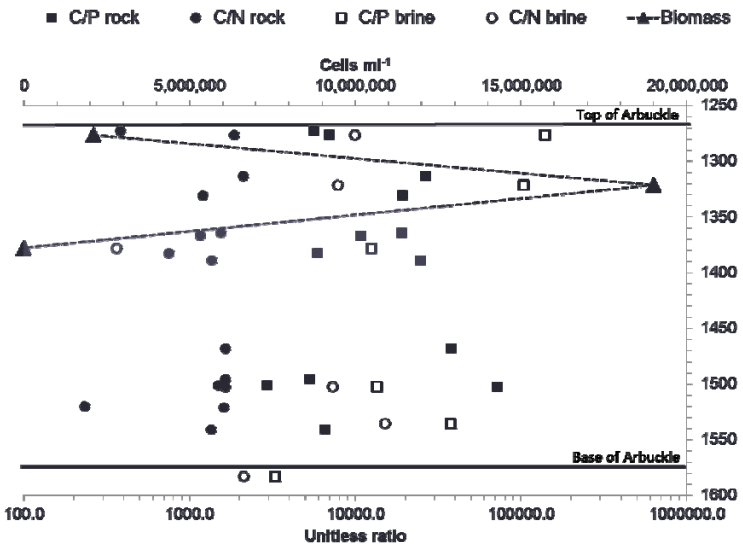

Figure 3.4. Carbon, nitrogen and phosphorus elemental analysis for reservoir rocks and brine for Wellington oil field in Sumner county, Kansas. Nitrogen concentrations are relatively steady in contrast with more variable carbon and phosphorus. The nutrient values of the brine from 1378 m depth coincide with a decreased DOC, high nitrogen, low phosphorus and a decrease in biomass and is located within the low permeability and high impedance zone of the lower JCC formation.

Microbial Diversity The free-living microbial community was examined in the Upper Arbuckle saline aquifer. Results show 43% diversity at a depth of 1277 m, 62% diversity at 1321 m, and 39% diversity at 1378 m, which follows the same trend as biomass (Fig. 3.5). Notably, the microbial communities from 1277 m and 1321 m are very similar to one another and vary distinctly from the community detected at 1378 m. The same nine genera of Bacteria were detected at 1277 m and 1321 m; *Alkalibacter, Alkaliflexus, Bacillus, Clostridiales*, *Cyclobacteriaceae, Erysipelthrix, Halomonas, Marinilabiaceae*, and *Xylanimonas* (Fig. 3.5). Seven genera of Bacteria were detected at 1378 m (Fig. 3.5). *Alkalibacter, Bacillus and Erysipelthrix* were found at the two shallower depths but not at 1378 m. *Dethiobacter* was only detected at 1378 m. If a sequence did not match a phylum to 97% then it was considered unique and was not included on the graph, therefore all sequences presented on the graph match the

genus by 97% or better. Blast Sequence Analysis shows that 34 species were identified in brine from 1277 m, 49 from 1321 m, and 22 from 1378 m. The total richness of the three depths examined is 80 with a shared richness of 7. The species identified belong the orders *Bacteriodales, Firmicutes, Actinobacteria and Proteobacteria.* A table with more detail about the species identified, their accession numbers and diversity distributions can be found in the supporting materials (Table 3.1).

Diversity decreases notably at 1378 m and coincides with a decrease in DOC, which may indicate a dependence on organic carbon by heterotrophs in the reservoir. The highest biomass was detected at 1321 m, which is coincident with high concentrations of sulfate.

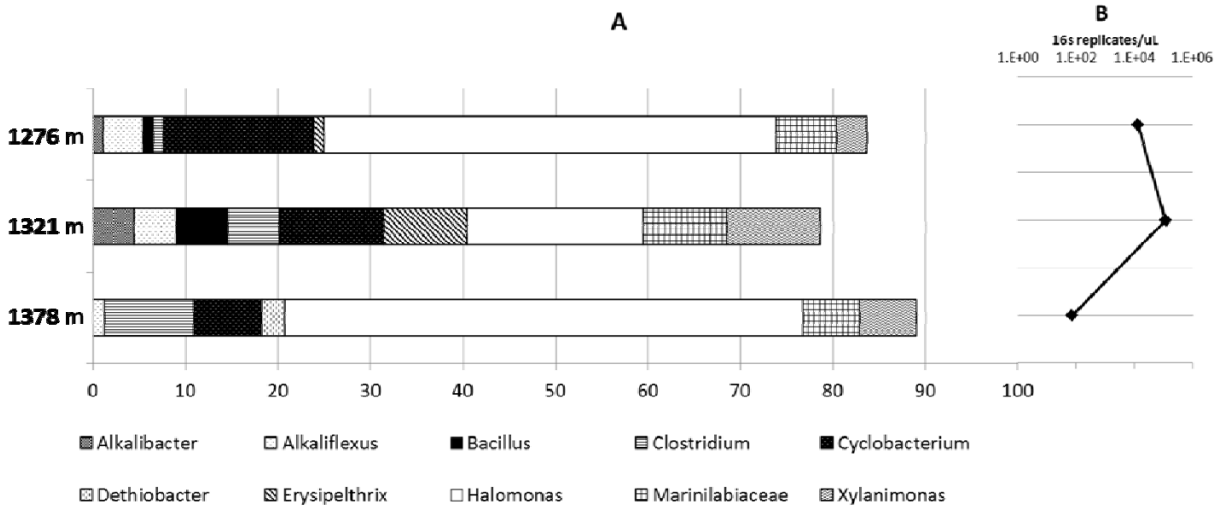

Figure 3.5. Arbuckle aquifer microbial profile showing the distribution of Bacteria in the Upper Arbuckle in Wellington oil field in Sumner county, Kansas (A). Nine genera of Bacteria were detected at 1277 m and 1321 m. Seven genera of Bacteria were detected at 1378 m. *Alkalibacter, Bacillus and Erysipelthrix* were found at the two shallower depths but not at 1378 m. *Dethiobacter* was detected only at the deeper depth of 1378 m. If a sequence did not match a phylum to 97% then it was considered unique and was not included on the graph, therefore all sequences presented on the graph match the genus by 97% or better. DNA concentration (B). The highest biomass and the most unique sequences occurred at 1321 m.

Fermentation was detected with culturing techniques in brine from 1332 m, 1486 m, 1502 m, 1527 m, 1582 m within the Arbuckle aquifer and granite basement. MPN estimated bacterial populations of 23 cells mL^{-1} in the waters from 1332 m, 1486 m, 1502 m, and 1527 m and 400

cells mL^{-1} at 1582 m. Fermentative bacteria produce hydrogen, which can in turn serve as the electron donor for methanogenesis and other metabolisms. Active iron reduction was also detected in brine from 1321 m and estimated an iron-reducing bacteria population of 13 cells mL^{-1}.

Sulfate reducers and methanogens were not detected in the brine via culturing. However, most sulfate reducers are typically *Firmicutes* or *Proterobacteria* (Lisa et al., 2011), which were detected with molecular methods and corresponds to a decrease in sulfate between 1321 m and the base of the reservoir confirming SRBs are present and active in the reservoir. Methanogens, nor any other archaea, were detected with molecular methods. This is not surprising because high sulfate levels in the Upper Arbuckle would almost guarantee SRBs would outcompete them. However, an increase in methane concentration, increased DOC concentrations and δC^{13} enrichment indicates autotrophic methanogens could be present at deeper levels in the reservoir. This could be confirmed with C^{13}/C^{12} fractionation comparison of CO_2 and CH_4 (Whiticar, 1998). Samples are currently being analyzed for $\delta C^{13}{}_{CH4}$ to help determine definitively if microbial methanogenesis is occurring in the reservoir.

Isotopic Characterization of Brine. Oxygen and hydrogen isotopes present another opportunity to assess hydraulic connectivity within the reservoir. Figure 3.6 shows the δD vs $\delta^{18}O$, reported as the difference between the $^{18}O/^{16}O$ and $^{2}H/^{1}H$ abundance ratios of the samples vs. the Vienna Standard Mean Ocean Water (VSMOW) in per mil notation ($^{o}/_{oo}$) for the Arbuckle saline aquifer and Mississippian oil producing reservoir samples collected for this study with best fit regression lines for each formation brine with the global meteoric water line (GMWL) (Craig, 1961) and modern seawater for comparison. The Mississippian samples were included to aid in the interpretation of the trend observed with the Arbuckle samples and to

discern geochemical separation between the two reservoirs. Mostly, the Arbuckle samples are enriched with depth with an exception occurring between 1276 m^{-1} 321 m. The brines from the Lower Arbuckle (1486 m^{-1} 535 m) cluster tightly together and have values distinct from those of the Upper Arbuckle (1277 m^{-1}378 m). The similarity of the brine from the Lower Arbuckle strongly suggests active communication between these depths in the reservoir. This confirms initial observations from core and well logs run in KGS 1-28 and KGS 1-32, which showed the reservoir was highly connected at these depths through an extensive network of connected small-scale solution enhanced fractures and vugs. The fractures are closely controlled by the original depositional fabric of autoclastic breccias and grainstones. For instance, the injection zone is a brecciated zone that was relatively easily correlated between the two wells.

In contrast to the Lower Arbuckle, the brines of the Upper Arbuckle show more variability (Fig. 3.6). The Upper Arbuckle brines from 1276 and 3121 m have distinctly different δD and $\delta^{18}O$ values from everything below but are significantly different than the Lower Arbuckle. The trend of δD and $\delta^{18}O$ values of 1277 m and 1321 m are decreasing with depth which is a different trend than is observed with samples from every other depth. This difference in the Upper Arbuckle is indicative of an influx of more isotopically enriched waters from another brine or meteoric waters. This suggests the Upper Arbuckle is in communication with the units above to some degree and suggests that the Lower Arbuckle is not connected to the Upper Arbuckle.

To explore this possibility, the regression line of the Mississippian samples was extended to show the relationship to the Upper Arbuckle samples but is calculated exclusively using the three Mississippian samples. The slopes of the GMWL, and best-fit regression lines of the Arbuckle and Mississippian values are 8.0, 8.3, and 6.7 respectively. The trend of the δD and

$\delta^{18}O$ of Mississippi would allow for a reasonable fit to the Upper Arbuckle samples, which would support the theory that those units are to some extent connected, however, the chlorine data discussed below strongly refutes this possibility. Although, an isotope study by Degens et al. (1963) in Osage County, Oklahoma and very near our study area did conclude that the Upper Arbuckle appeared to be in pressure communication with the lower Simpson formation leading to free interchange of formation fluids between them. It is also interesting to note that in contrast to the Mississippian brines, the Arbuckle brines are trending toward modern seawater with depth suggesting the origin can at least in part be contributed to connate waters (Dowgiallo, 1975).

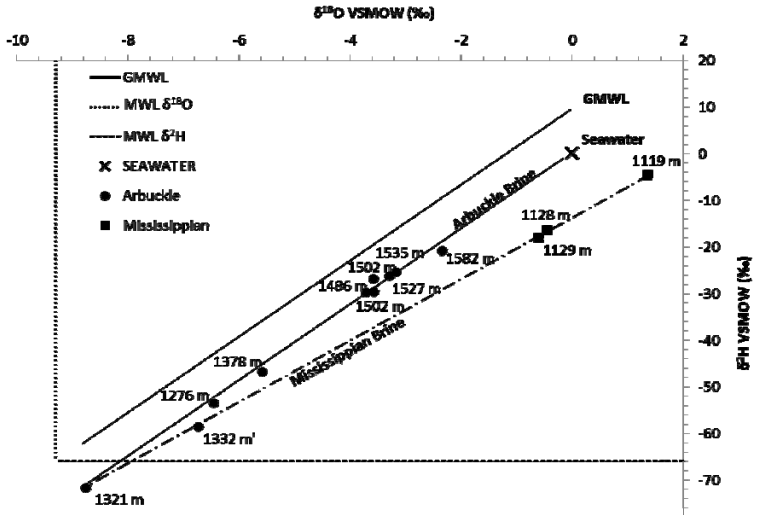

Figure 3.6. δD vs $\delta^{18}O$ ($^{o}/_{oo}$, VSMOW) for the Arbuckle saline aquifer and Mississippian oil producing reservoir samples from Wellington oil field in Sumner County, Kansas. Also shown are the best fit regression lines for each formation brine, the global meteoric water line (Craig, 1961), and modern day seawater for comparison. The brines from the Lower Arbuckle (1486 m^{-1}535 m) group tightly together and are easily distinguished from those of the Upper Arbuckle (1277 m^{-1}378 m). The regression line of the Mississippian samples was extended to show the relationship to the Upper Arbuckle samples but is calculated exclusively using the three Mississippian samples. There an increase in enrichment with increasing depth for the Arbuckle samples with an exception occurring between 1277 m^{-1}321 m. The slopes of the GMWL, and best-fit regression lines of the Arbuckle and Mississippian values are 8.0, 8.3, and 6.7 respectively.

Ion concentrations have been used extensively to examine the origin and mixing of basinal brines by Rittenhouse (1967), Musgrove and Banner (1993), Richter and Kreitler (1987), Whittemore (2007), Davisson et al. (1996), Chi and Martine (1995), and Davis et al. (1998) and others. Due to their conservative nature during water rock interactions with carbonates and

silicates, bromine and chlorine are especially useful in differentiating salinity sources and detecting brine mixing (Whittemore, 1995) the latter being the goal herein. Bromine, chlorine, and sulfate concentrations of brine from 9 depths in the Arbuckle and 3 depths in the Mississippian formations were evaluated. The Br^-/Cl^- and SO_4^{2-}/Cl^- weight ratios versus chloride concentration for the Arbuckle saline aquifer and Mississippian oil producing brines in Wellington oil field in Sumner County, Kansas are presented in Figure 3.7.

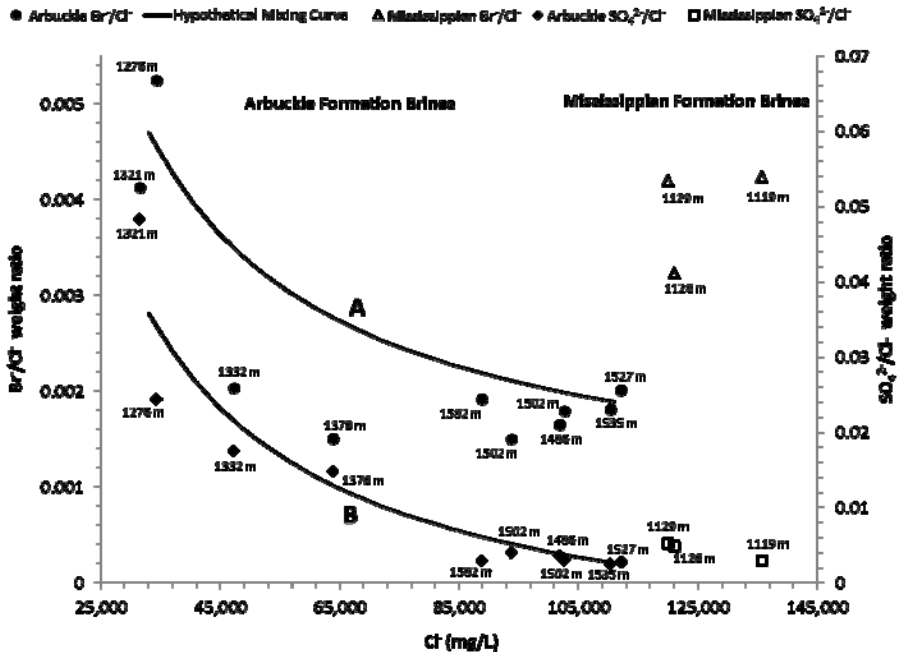

Figure 3.7. Br^-/Cl^- and SO_4^{2-}/Cl^- weight ratios versus chloride concentration for the Arbuckle saline aquifer and Mississippian oil producing brines in Wellington oil field in Sumner County, Kansas. Also shown are the hypothetical mixing curves for mixing between Lower Arbuckle brine and Upper Arbuckle brine are shown for both Br^-/Cl^- (A) and SO_4^{2-}/Cl^- (B) versus chloride. Comparison of the Br^-/Cl^- data from the Upper and Lower Arbuckle to the mixing line support that the brines from 1321 m and 1277 m are distinctly different and do not undergo mixing with the fluids below (A). The SO_4^{2-}/Cl^- values fall closer to the mixing line up to 1332 m indicating some mixing between 1332 m, 1321 m, and the Lower Arbuckle. The high sulfate concentrations of 1277 m and 1321 m in the Upper Arbuckle continue to support the idea that these two depths are not in fluid communication with the Lower Arbuckle

Br^-/Cl^- ratios of 0.0002 to 0.0052 and chloride concentrations of 31,000 mg L^{-1} to 137,000 mg L^{-1} were observed with the highest salinities occurring in the in the shallower Mississippian formation (Fig. 3.7). The Br^-/Cl^- values of the Lower Arbuckle vary nominally from 0.0015 and 0.0020. The Cl^- values of the Lower Arbuckle diverge slightly more from about 89,000 to 112,000 mg L^{-1}. The Br^-/Cl^- values of the Upper Arbuckle vary substantially

more, from 0.0015 and 0.005, than values observed in the Lower Arbuckle. The Cl^- values of the Upper Arbuckle range from about 31,000 to 64,000 mg L^{-1}. Chlorine increases almost linearly with depth within the Arbuckle aquifer so bromine is dictating the observed trends. A hypothetical mixing curve was calculated using end-member values averaged from the two deepest samples in the Arbuckle (1527 m and 1535 m) and the two shallowest samples in the Arbuckle (1277 m and 1321 m) to examine mixing of reservoir fluids to evaluate connectivity throughout the reservoir. The Lower Arbuckle samples display a curious trend with Br^-/Cl^- initially decreasing through the middle Arbuckle and then increasing sharply in the Upper Arbuckle. This could suggest there may be different brine origins causes the difference in Bromine concentrations between the Lower and Upper Arbuckle. One explanation would be if the brine source of the Lower Arbuckle was a combination of seawater evaporation and halite dissolution and the source of the Upper Arbuckle had been diluted with fresh water, which tends to have higher levels of bromine (Rittenhouse, 1967). Regardless, these data support that the brines from 1321 m and 1277 m are distinctly different that the other reservoir fluids and do not undergo mixing with the fluids below. Therefore, the bromine/chlorine data in Figure 3.7 supports isotope data in suggesting that the Lower Arbuckle is likely not in hydraulic communication with the Upper Arbuckle. Additionally, these data point towards hydrologic separation of 1378 m and 1332 m from the brines both in the Upper and Lower Arbuckle suggesting the presence of a Middle Arbuckle hydrologic zone. Br^-/Cl^- values of the Mississippian oil producing reservoir are easily distinguished from Arbuckle brines although they reflect similar Br^- values to the Upper Arbuckle but with clear distinction based on the high chloride concentration indicating there is not communication between these units. Isotopes fractionation can be influenced by various interactions with the reservoir, like clay and

temperature (Ziegler and Longstaffe, 1999), but bromine and chlorine are very conservative ions (Whittemore, 1995). Therefore, the Br^-/Cl^- ratios may allow for a more accurate interpretation of connectivity.

SO_4^{2-}/Cl^- ratios of 0.02 to 0.07 were observed (Fig. 3.7). The SO_4^{2-}/Cl^- values of the Lower Arbuckle show a similar trend as the Br^-/Cl^- in that they vary nominally from 0.0024 and 0.0040. The SO_4^{2-}/Cl^- values of the Upper Arbuckle vary substantially more, from 0.015 and 0.048, than values observed in the Lower Arbuckle. A hypothetical mixing curve was calculated using end-member values from the same depths as with bromine to examine mixing of reservoir fluids to evaluate connectivity throughout the reservoir. Unlike the bromine data, the sulfate data falls closer to the hypothetical Upper and Lower Arbuckle mixing line somewhat until a depth of 1332 m suggesting there could be some mixing between 1332 m, 1378 m and the Lower Arbuckle. However, the errant sulfate concentrations of 1277 m and 1321 m in the Upper Arbuckle continue to support the idea that these two depths are not in hydraulic communication with the Lower Arbuckle. These data corroborate with the log, core, seismic, geochemical, microbiological, isotopic, and anion ratio results which all point to hydraulic separation of the Upper and Lower Arbuckle. Therefore, CO_2 injection should occur in the Lower Arbuckle to take advantage of the accelerated pore space trapping and dissolution benefits provided by the baffle.

Acknowledgements

Material presented is based upon work supported by the U.S. Department of Energy (DOE) National Energy Technology Laboratory (NETL) under Grant Number DEFE0000002056. This project is managed and administered by the Kansas Geological Survey/KUCR, W. L. Watney, PI, and funded by DOE/NETL and cost-sharing partners.

Disclaimer: This report was prepared as an account of work sponsored by an agency of the United States Government. Neither the United States Government nor any agency thereof, nor any of their employees, makes any warranty, express or implied, or assumes any legal liability or responsibility for the accuracy, completeness, or usefulness of any information, apparatus, product, or process disclosed, or represents that its use would not infringe privately owned rights. Reference herein to any specific commercial product, process, or service by trade name, trademark, manufacturer, or otherwise does not necessarily constitute or imply its endorsement, recommendation, or favoring by the United States Government or any agency thereof. The views and opinions of authors expressed herein do not necessarily state or reflect those of the United States Government or any agency thereof.

We thank Masato Ueshima for assistance with cation and anion analyses and Greg Kane of Keck Paleo-Environmental Stable Isotope Laboratory for preparation of reference samples used in isotopic analyses. We thank Jason Bruns of Berexco LLC, Mark Villarreal and Breanna Huff of the University of Kansas for their assistance in the field. This research was supported by the U.S. Department of Energy (DOE), Kansas Geological Survey, DOSECC, Rocky Mountain Federation of Mineralogic Societies, Kansas Geological Society, and the Association for Women Geoscientists.

References

Abdulla, H., (2009). Bioweathering and Biotransformation of Granitic Rock Minerals by Actinomycetes. Microbial Ecology. 58, 4: 753-761.

Alkan, H., Cinar, Y., and Ulker, E.B., (2010). Impact of Capillary Pressure, Salinity and In situ Conditions on CO_2 Injection into Saline Aquifers. Transport in Porous Media. 84, 3: 799-819.

Amy, P.S., Haldeman, D. L., (1997). The microbiology of the terrestrial deep subsurface. The microbiology of extreme and unusual environments: 356.

Bacci, G., Korre, A., and Durucan, S., (2011). An experimental and numerical investigation into the impact of dissolution/precipitation mechanisms on CO_2 injectivity in the wellbore and far field regions. International Journal of Greenhouse Gas Control. 5, 3: 579-588.

Bachu, S., (2002). Sequestration of CO_2 in geological media in response to climate change: road map for site selection using the transform of the geological space into the CO_2 phase space. Energy Conversion and Management. 43, 1: 87-102.

Bachu, S. and Bennion, B., (2008). Effects of in-situ conditions on relative permeability characteristics of CO_2-brine systems. Environmental Geology. 54, 8:1707-1722.

Beveridge, T. J., (1989). Role of Cellular Design in Bacterial Metal Accumulation and Mineralization. Annual Review of Microbiology, 43, 1: 147-171.

Carr, J.E., McGovern, H. E., Gogel, T., (1986). Geohydrology of and potential for fluid disposal in teh Arbuckle Aquifer in Kansas. U.S. Geological Survey open-file report, 86-491: 87.

Carr, T.R., Merriam, D.F., and Bartley, J.D., (2005). Use of relational databases to evaluate regional petroleum accumulation groundwater flow, and CO_2 sequestration in Kansas. AAPG Bulletin. 89, 12:1607-1627.

Chi, G. and Savard, M.M., (1997). Sources of basinal and Mississippi Valley-type mineralizing brines: mixing of evaporated seawater and halite-dissolution brine. Chemical Geology. 143, 3–4:121-125.

Craig, H., (1961). Isotopic Variations in Meteoric Waters. Science. 133, 346: 1702.

Croal, L.R., (2004). The genetics of geochemistry. Annual Review of Genetics. 38: 175-202.

Daneshfar, J., Hughes, R.G., and Civan, F., (2009). Feasibility Investigation and Modeling Analysis of CO_2 Sequestration in Arbuckle Formation Utilizing Salt Water Disposal Wells. Journal of Energy Resources Technology-Transactions of the Asme. 131, 2.

Davis, S.N., Whittemore, D.O. and Fabryka-Martin, J., (1998). Uses of chloride/bromide ratios in studies of potable water. Ground Water. 36, 2: 338-350.

Davisson, M.L. and Criss, R.E., (1996). Na-Ca-Cl relations in basinal fluids. Geochimica et Cosmochimica Acta. 60, 15: 2743-2752.

Degens, E.T., (1964). Data on the Distribution of Amino Acids and Oxygen Isotopes in Petroleum Brine Waters of Various Geologic Ages. Sedimentology. 3, 3: 199-225.

Dickey, P.A., (1966). Patterns of chemical composition in deep subsurface waters. American Association of Petroleum Geologists Bulletin. 50, 11: 2478.

Dowgiallo, J., (1971). Stable Isotopes as Indicators of the Origin and Zonal Affiliation of Deep-Seated Ground Waters in Sedimentary Basins, Centre de Recherches Geologiques, Academie Polonaise des Sciences, 562-568

Ehrlich HL (1996) Geomicrobiology. Dekker, New York.

Emberley, S., (2004). Geochemical monitoring of fluid-rock interaction and CO_2 storage at the Weyburn CO_2-injection enhanced oil recovery site, Saskatchewan, Canada. Energy. 29, 9-10: 1393-1401.

Emberley, S., (2005). Monitoring of fluid-rock interaction and CO_2 storage through produced fluid sampling at the Weyburn CO_2-injection enhanced oil recovery site, Saskatchewan, Canada. Applied Geochemistry. 20, 6: 1131-1157.

Franseen, E.K., Byrnes, A. P., (2004). The geology of Kansas: Arbuckle Group. Kansas Geological Survey Bulletin. 250, 2: 43.

Ghojavand, H., (2008). Isolation of thermotolerant, halotolerant, facultative biosurfactant-producing bacteria. Applied Microbiology and Biotechnology. 80, 6: 1073-1085.

Gieg, L.M., Jack, T.R. and Foght, J.M., (2011). Biological souring and mitigation in oil reservoirs. Applied Microbiology and Biotechnology. 92, 2: 263-282.

Jacobson, A.D. and Wu, L., (2009). Microbial dissolution of calcite at T =28°C and ambient pCO_2. Geochimica et Cosmochimica Acta. 73, 8: 2314-2331.

Jorgensen, D.G., Helgesen, J. O., Imes, J. L., (1993). Regional Aquifers in Kansas, Nebraska, and parts of Arkansas, Colorado, Missouri, New Mexico, Oklahoma, South Dakota, Texas, and Wyoming- geohydrologica framework. Regional aquifer-system analysis-Central Midwest 1414-B: 72.

Kashefi, K. and Lovley, D.R., (2003). Extending the upper temperature limit for life. Science. 301, 5635: 934-934.

Kaszuba, J.P., Janecky, D.R. and Snow, M.G., (2003). Carbon dioxide reaction processes in a model brine aquifer at 200 degrees C and 200 bars: implications for geologic sequestration of carbon. Applied Geochemistry. 18, 7: 1065-1080.

Kaszuba, J.P., Janecky, D.R. and Snow, M.G., (2005). Experimental evaluation of mixed fluid reactions between supercritical carbon dioxide and NaCl brine: Relevance to the integrity of a geologic carbon repository. Chemical Geology. 217, 3-4: 277-293.

Ketzer, J.M., (2009). Water-rock-CO_2 interactions in saline aquifers aimed for carbon dioxide storage: Experimental and numerical modeling studies of the Rio Bonito Formation (Permian), southern Brazil. Applied Geochemistry, 2009. 24, 5: 760-767.

Kharaka, Y.K., (2006). Gas-water-rock interactions in Frio Formation following CO_2 injection: Implications for the storage of greenhouse gases in sedimentary basins. Geology. 34, 7: 577-580.

Kharaka, Y.K., et al., Gas-water-rock interactions in Frio Formation following CO_2 injection: Implications for the storage of greenhouse gases in sedimentary basins. Geology, 2006. 34(7): p. 577-580.

Kharaka, Y.K., (2009). Potential environmental issues of CO_2 storage in deep saline aquifers: Geochemical results from the Frio-I Brine Pilot test, Texas, USA. Applied Geochemistry. 24, 6: 1106-1112.

Kneafsey, T.J. and Pruess, K., (2011). Laboratory experiments and numerical simulation studies of convectively enhanced carbon dioxide dissolution. Energy Procedia. 4, 0: 5114-5121.

Lin, H., (2008). Experimental evaluation of interactions in supercritical CO_2/water/rock minerals system under geologic CO_2 sequestration conditions. Journal of Materials Science. 43, 7: 2307-2315.

Lu, P., (2011). Navajo Sandstone-brine-CO_2 interaction: implications for geological carbon sequestration. Environmental Earth Sciences. 62, 1: 101^{-1}18.

Luquot, L. and Gouze, P., (2009). Experimental determination of porosity and permeability changes induced by injection of CO_2 into carbonate rocks. Chemical Geology. 265, 1-2: 148-159.

Magot, M., Ollivier, B. and Patel, B.K.C., (2000). Microbiology of petroleum reservoirs. Antonie Van Leeuwenhoek International Journal of General and Molecular Microbiology. 77, 2: 103-116.

Marion, G.M., (2003). The search for life on Europa: Limiting environmental factors, potential habitats, and Earth analogues. Astrobiology. 3, 4: 785-811.

Min, J.-E., (2009). Effect of phosphate and sediment bacteria on trichloroethylene dechlorination with zero valent iron. Journal of Environmental Science & Health, Part A: Toxic/Hazardous Substances & Environmental Engineering. 44, 4: 362-369.

Morozova, D., (2010). Monitoring of the microbial community composition in saline aquifers during CO_2 storage by fluorescence in situ hybridisation. International Journal of Greenhouse Gas Control. 4, 6: 981-989.

Morozova, D., (2011). Monitoring of the microbial community composition in deep subsurface saline aquifers during CO_2 storage in Ketzin, Germany. Energy Procedia. 4, 0: 4362-4370.

Musgrove, M. and Banner, J.L., (1993). Regional ground-water mixing and the origin of saline fluids: Midcontinent, United States. Science. 259, 5103: 1877.

Newell, D.K., (1987). Stratigraphic and spatial distribution of oil and gas production in Kansas. Subsurface geology series. 9, 1: 86.

Pedersen, K., (2000). Exploration of deep intraterrestrial microbial life: current perspectives. Fems Microbiology Letters. 185, 1: 9-16.

Prigiobbe, V., (2009). The effect of CO_2 and salinity on olivine dissolution kinetics at 120 degrees C. Chemical Engineering Science. 64, 15: 3510-3515.

Rhodes, M.E., (2010). Amino acid signatures of salinity on an environmental scale with a focus on the Dead Sea. Environmental Microbiology. 12, 9: 2613-2623.

Richter, B.C. and Kreitler, C.W., (1987). Sources of Groundwater Salinization in Parts of West Texas. Ground Water Monitoring and Remediation. 7, 4: 75-84.

Rimmele, G., (2008). Heterogeneous porosity distribution in Portland cement exposed to CO_2-rich fluids. Cement and Concrete Research. 38, 8-9: 1038-1048.

Rittenhouse, G., (1967). Bromine in oil-field waters and its use in determining possibilities of origin of these waters. American Association of Petroleum Geologists Bulletin. 51, 12: 2440.

Roberts, J.A., (2004). Microbial precipitation of dolomite in methanogenic groundwater. Geology. 32, 4: 277-280.

Sharma, A., (2002). Microbial activity at gigapascal pressures. Science. 295, 5559: 1514-1516.

Shock, E.L., (2009). Minerals as Energy Sources for Microorganisms. Economic Geology. 104, 8: 1235-1248.

Walters, R.F., (1958). Differential entrapment of oil and gas in Arbuckle dolomite of central Kansas. American Association of Petroleum Geologists Bulletin. 42, 133-2: 173.

Wandrey, M., (2011). Microbial community and inorganic fluid analysis during CO_2 storage within the frame of CO_2SINK–Long-term experiments under in situ conditions. Energy Procedia. 4, 0: 3651-3657.

Wang, L. Miller, T.D., Priscu, J.C., (1992). Bacterioplankton nutrient deficiency in a eurtrophic lake. Arch. Hydrobiology. 125: 423-439.

Watney, L.W., French, J., (1988). Missourian (upper Pennsylvanian) Lansing and Kansas City groups in the Kansas city area - mixed carbonate-clastic sequences. Kansas Geological Survey open-file report. 88-41, 1: 60.

Welch, S.A. and Vandevivere, P., (1994). Effect of microbial and other naturally occurring polymers on mineral dissolution. Geomicrobiology Journal. 12, 4: 227-238.

Whiticar, M.J., (1999). Carbon and hydrogen isotope systematics of bacterial formation and oxidation of methane. Chemical Geology. 161, 1-3: 291-314.

Whittemore, D.O., (2007). Fate and identification of oil-brine contamination in different hydrogeologic settings. Applied Geochemistry. 22, 10: 2099-2114.

Wigand, M., (2008). Geochemical effects of CO_2 sequestration in sandstones under simulated in situ conditions of deep saline aquifers. Applied Geochemistry. 23, 9: 2735-2745.

Wu, L., Jacobson, A.D. and Hausner, M., (2008). Characterization of elemental release during microbe–granite interactions at T =28°C. Geochimica et Cosmochimica Acta. 72, 4: 1076-1095.

CHAPTER 4

Geochemical and Microbiological Influences on Seal Integrity During SC-CO_2 Exposure, Arbuckle aquifer, SE Kansas

ABSTRACT

The Kansas Geological Survey is evaluating the potential of the Arbuckle dolomite for CO_2 sequestration, as well as the potential of the Mississippi "lime" for CO_2 enhanced oil recovery (EOR) across Southern Kansas which necessitates examination of the reservoir seals. Therefore, a series of batch experiments were performed to evaluate the geochemical and microbiological influences of CO_2 injection on reservoir materials and seal integrity of the Cherokee and Chattanooga Shales, which are currently considered the primary seals of these two reservoirs. These rocks as well as single mineral experiments were performed with native brines at reservoir temperatures and pressures with 100% pCO_2.

Aqueous geochemistry, XRD and SEM conducted on the experiment products confirmed mineralogical changes occurred in experiments containing pyrite and Chattanooga Shale after CO_2 exposure. XRD did not indicate that mineralogical changes occurred in experiments with dolomite or Cherokee Shale. However, aqueous geochemical data showed considerable changes were occurring in these experiments as well. It is likely that materials in these experiments incompletely dissolved or precipitates were below detection using XRD. No significant differences between biotic and abiotic experiments were observed, possibly due to low biomass in the reservoir.

Mineralogic changes to seal and reservoir minerals induced by CO_2 exposure significantly impact water:rock:microbe interactions and have implications for maintaining reservoir porosity and permeability in these systems. Our results suggest that pyrite-bearing phases may precipitate secondary gypsum in the presence of CO_2 and oxygenated brine fluids.

Gypsum precipitation under these conditions could fill existing pore space or micro-fractures within the seals to create an even better seal, or conversely clog CO_2 storage pore space, lowering storage capacity of the reservoir. Potentially even more detrimental would be precipitation of these minerals near injection, a likely location for oxygenation, resulting in a decrease of injection capability.

Introduction

The Kansas Geological Survey is evaluating the potential of the Arbuckle dolomite for CO_2 sequestration, as well as the potential of the Mississippi "lime" for CO_2 enhanced oil recovery (EOR) across southern Kansas. Carbon sequestration is the process of capturing carbon from power plants and depositing it into underground reservoirs. In the case of CO_2 EOR, the underground reservoir is an oil field where the solvent properties of the injected CO_2 increase oil production and can considerably decrease the percentage of oil left in place. Geologic storage of carbon is proving to be an increasingly feasible option, however every GCS site is unique and must undergo detailed characterization prior to injection. Some critical parameters to qualify a reservoir as a feasible GCS site is a large storage capacity, injectivity and an effective, regionally extensive seal. Therefore, it is imperative to characterize the reservoir system and demonstrate the integrity of the reservoir and seals.

Much of the existing research has been performed in batch laboratory reactions at ambient pressures with varying temperature with systems saturated with carbon dioxide. Due to the unique properties of supercritical fluids, it is important to conduct studies with CO_2 in the supercritical phase to properly model the potential geochemical reactions. Work by Kaszuba et al. (2003, 2005), Kharaka et al. (2009), Wigand et al. (2008) and others have examined geochemical effects of brine and supercritical CO_2 on reservoir rocks at temperatures and

pressures analogous to reservoir conditions. For instance Kaszuba et al. (2003) found a diversity of fluid-rock reactions in addition to carbonate precipitation occurred in their experiments. Silicate minerals, and shales displayed textures suggesting they reacted strongly with the fluid, as well as dramatic changes in brine chemistry. Experiments conducted by Kaszuba et al. (2005) confirmed that shales and other aquitard rock units react strongly when injected with $CO_{2(sc)}$ reiterating the relevance of these studies to predict, and potentially avoid, integrity problems with the carbon storage formation and caprocks. The general consensus in the literature is that the dominant reaction after injection of CO_2 will be rapid dissolution due to increased acidity. Unfortunately, the desired result of carbon sequestration is mineral formation (carbonation), which is a secure, long term (millions of years) storage of the CO_2. But getting the minerals to precipitate away from injection is needed and requires the pH to decrease. Extensive research on mineral trapping has been conducted by Gunter et al. (2004), Daval et al. (2009), Dufaud et al. (2009) Keleman and Matter (2008) and others. However, all of these experiments failed to include a microbial component in their studies.

The studies of rock-brine-CO_2 interactions indicate complex geochemical interactions are occurring, usually involving both precipitation and dissolution reactions. For example, Lu et al. (2011) found that silicate dissolution was the dominant reaction when CO_2 was reacted with the Navajo sandstone but several authigenic clays were produced. These studies illustrate why it is vital to understand the complex geochemical processes at work in each system in order to predict success, project realistic storage estimates and injection rates, and also to provide realistic data for widely applied reactive transport models. Untimely precipitation can lead to clogging of the well materials or of the aquifer itself near the point of injection. This could render the injection well useless or cause expensive material repair and upkeep. On the other hand, rapid dissolution

can lead to storage integrity concerns with well bores, well cements and cap rocks. Shales are common components in cap rock systems. Experiments by Kaszuba et al. (2003) showed that shales actively participate in fluid-rock interactions in CO_2 storage systems. This is relevant to many carbon storage reservoirs that have shale components in the cap rock system and could lead to serious storage integrity concerns and possibly drinking water contamination in overlying freshwater aquifers.

Although the research discussed is diverse, the parameter they consistently neglect to address is microorganisms of which the importance of their metabolic activity to geochemical equilibria reactions was outlined in previous chapters. However, CO_2 is known to have deleterious effects on a number of microorganisms. In fact, it is extensively used by the food industry for treatment of dairy products, preservation of meat and fish, prevention of food spoilage etc. as discussed in the review paper by Dixon et al. (1989). Although CO_2 is used in a wide variety of applications to kill bacteria, sterilization is rarely achieved (Dixon et al., 1989). The known effects of CO_2 on bacterial communities suggest that large populations of microorganisms may die when carbon dioxide is injected into the subsurface which would result in a release of organic carbon (Dixon and Kell, 1989). Organic carbon in highly reactive geochemically, therefore the introduced organic carbon could buffer the pH, act as a proton donor, or absorb cations, all which could impact precipitation and dissolution reactions (Weishaar et al., 2003). This is particularly relevant around the wellbore where CO_2 will be at the highest concentrations and therefore the most damaging to the microbial community. The introduction of CO_2 will cause disequilibrium around the wellbore, which will be exacerbated by dissolved organic carbon (DOC) released from bacterial lysis, which needs to be examined experimentally. Therefore, the experiments discussed herein explored the effects of DOC

released from cell lysis of the native microbial population on geochemical reactions between seal materials and reservoir brine during CO_2 exposure in high pressure and temperature batch experiments to assess seal integrity on the two most essential seals associated with these reservoirs; 1) the Chattanooga Shale, the primary seal of the Arbuckle aquifer, and 2) the Cherokee Shale, secondary seal of the Arbuckle aquifer and primary seal of the Mississippian reservoir. In order to remove some of the complexity, a set of single-mineral phase experiments were also performed. Dolomite and pyrite were selected because of their abundance in the seals and reservoir rock.

Methods

Field sampling methods and geochemical analyses of "pre" samples used in all batch experiments can be referenced in Chapter 3 of this thesis. A series of six batch experiments were done to evaluate the geochemical and microbiological influences on seal integrity and reservoir injectivity utilizing the Cherokee and Chattanooga shales and single mineral phases of pyrite and dolomite. Pyrite and dolomite were selected because they are abundant minerals in both the reservoir and seal formations and were expected to be two of the most reactive minerals of the reservoir and seal mineralogy. Pore fluids, with native microbial consortia, were collected from the Arbuckle and Mississippian aquifers from a series of drill-stem-tests during drilling of KGS #1-28 and KGS #1-32. Seal materials were selected from the KGS #1-32 core (see Chapter 3) and minerals were obtained from Wards "Dolomite Research Mineral" Order #49 V 5871, and "Pyrite (Best Grade), 1kg bulk pack", Order #46 V 6418**.**

The seal materials and minerals were powdered and sieved to the 63-150 μm size-fraction, and rinsed with DI water to remove the finer grain materials, then air dried. Ten grams of crushed seal material was then combined with 250-ml of reservoir fluids and placed into a 1.3-

liter steel autoclave reactor vessel lined with a Teflon liner which was then pressurized and heated to average reservoir temperature and pressure (2500 psi and 50°C). After purging, the vessels were filled with 100% pCO_2 super-critical CO_2 using a high-precision Teledyne ISCO pump and allowed to sit at constant temperature and pressure for the duration of each experiment. Five time-sequence experiments were conducted for each shale; 5, 7, 14, 30, and 45 days and the single-mineral experiments were conducted for 15 days with either pyrite or dolomite.

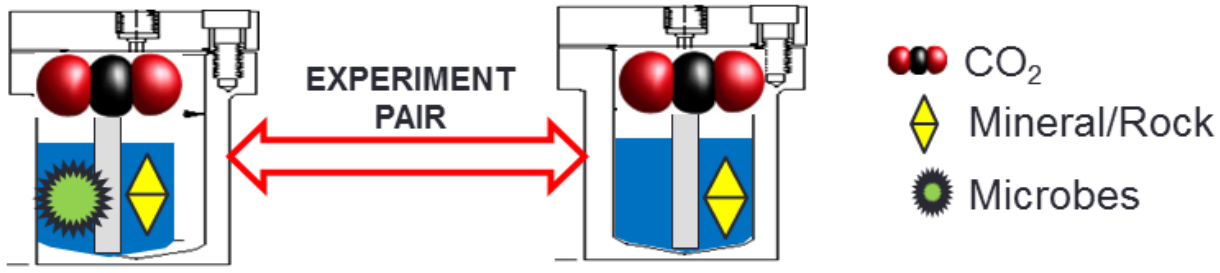

Figure 4.1. Experimental design of high pressure and high temperature batch experiments showing paired biotic/abiotic experiments with supercritical CO_2, minerals and reservoir brine with and without the presence of microbes. Each vessel contained either powdered caprock material or a single mineral phase.

Experiments were conducted in biotic and abiotic pairs to discern microbial impacts on the system. The brine used in the biotic experiments was raw production water, while the abiotic experiments used the same fluids after filtering through a 0.2 µm filter. Brine geochemistry was analyzed before and after each experiment (see detailed methods in Chapter 3) and solids were analyzed with XRD and SEM.

XRD powder patterns were collected using monochromated CuKα radiation (λ= 1.54178 Å) on a Bruker Proteum Diffraction System equipped with Helios high-brilliance multilayer optics, a Platinum 135 CCD detector and a Bruker MicroStar microfocus rotating anode x-ray source operating at 45kV and 60mA. Reacted and "pre" powders where prepared for SEM using critical point drying by serially increasing the concentration of an ethanol solvent to 100%

(Vandevivere, 1994). Each sample was placed in a small holding chamber fitted with 0.2µM filter to ensure no materials were lost during the drying. The dried samples were transferred on to an aluminum stub and gold coated using a Sputter Coater operated at 5mA for 3 minutes. The stubs were loaded into Leo 1550 Field Emission Scanning Electron microscope and imaged at a voltage of 10kV. Raw reservoir fluids were stored in the refrigerator for 8-12 months before being used in these experiments. Microbial biomass was quantified using the Quant-iT™ PicoGreen® dsDNA and were carried out following the protocol as outlined in the Quant-iT™ PicoGreen® dsDNA kit by Invitrogen. PhreeqC was used to examine saturation phases for all minerals in the system (Parkhurst, 1995).

Experiment	Brine depth	Rocks/Minerals	Duration
1	4335’	Cherokee shale (3569’) Chattanooga Shale (4065’)	45 days
2	4335’	Pyrite Dolomite	15 days
3	4118’	Cherokee shale (3569’) Chattanooga Shale (4088’)	30 days
4	4118’	Cherokee shale (3569’) Chattanooga Shale (4088’)	14 days
5	4520’	Cherokee shale (3584’) Chattanooga Shale (4088’)	7 days
6	5037’	Cherokee shale (3584’) Chattanooga Shale (4088’)	5 days

Table 4.1. Table showing the duration and materials used for each batch experiment.

Aqueous Geochemistry

Prior to CO_2 exposure

The brine chemistry was analyzed before and after each CO_2 exposure for each material. Extensive changes in brine chemistry were observed after CO_2 exposure of each material. Due to limited sample availability, brine from different depths (with slightly different chemistries) had to be used in each experiment, therefore the results are presented as change from the “pre” concentration for each constituent in the brine. Data for all of the experiments is included in the

appendices, however the focus here will be on the results of the 14 and 30 days shale experiments and the 15 day pyrite experiment.

Brine collected from 1276 m was used in the Cherokee and Chattanooga shale batch experiments and brine collected from 1321 m was used for the single-mineral (pyrite and dolomite) experiments. In situ temperature of the reservoir at these depths was 43.9°C to 50.3 °C and in situ pH of 6.9 and 7.1 respectively.

Brine data

Depth (m)	T °c	pH (field)	HCO_3	DOC	CH_4	Br	Cl	N/NO_3	P/PO_4	SO_4	$\delta^{13}C_{DIC}$ VPDB (‰)	Be
1276	43.9	7.1	6.2	12	7.E-01	1.1	969	0.07	8.42E-05	8.4	-24.4	17
1321	46.0	6.9	6.6	11	7.E-01	0.9	889	0.09	1.05E-04	15.3	-22.7	17

Depth (m)	Ca	K	Mg	Na	B	Sl	Fe^{2+}	Fe total	Al	Sr	$\delta^{18}O$ VSMOW (‰)	$\delta^{2}H$ VSMOW (‰)
1276	61	6	22	805	12	0.1	0.4	0.2	0.1	3.7	-6.5	-53.6
1321	70	7	25	758	12	0.1	0.5	0.2	0.1	3.2	-8.8	-71.8

All values presented in mmol/L

Table 4.2. Brine chemistry of brine from the two depths used in shale batch experiments.

Results

Figure 4.4 and Table 4.3 illustrate the results of CO_2 exposure of brine and Cherokee Shale, Chattanooga Shale, or pyrite over 30 and 14 days for the shales and 15 days for pyrite. Values are shown as change in concentration in mmol L^{-1} of each constituent from the starting conditions of the brine. The difference between the Cherokee Shale results (gray), Chattanooga Shale results (brown) and pyrite results (pink) are clear.

Cherokee Shale

Samples used for experiments were collected from 1094.4 m (greenish gray calcareous shale) and 1092.4 m (medium dark gray shale with chert) from KGS 1-32 core. Dramatic changes in brine chemistry were observed after 14 and 30 day long exposure of the Cherokee shale to 100% pCO_2 (Fig. 4.2). pH decreased from 6.9 mmol L^{-1} to an average of 6.2 mmol L^{-1} after 14 days exposure and 5.9 after 30 days exposure (Fig. 4.2). Bicarbonate increased from 6.2 mmol L^{-1} to an average of 43.7 mmol L^{-1} after 14 days exposure and 45.5 mmol L^{-1} after 30 days

exposure. Notable increases in calcium, magnesium, potassium and sodium were also observed (Tab. 3). Calcium increased from 60.09 mmol L^{-1} 76.8 mmol L^{-1} after 30 days and 83 mmol L^{-1} after 14 days. Magnesium increased from 22.3 mmol L^{-1} 25.1 mmol L^{-1} after 30 days and 23.4 mmol L^{-1} after 14 days. Potasium increased from 6.3 mmol L^{-1} 7.4 mmol L^{-1} after 30 days and 6.9 mmol L^{-1} after 14 days. Sodium increased from 805 mmol L^{-1} 917 mmol L^{-1} after 30 days and 844 mmol L^{-1} after 14 days. Note that the initial changes increased with time. Although changes in the aqueous species were prominent, no discernible changes in bulk mineralogy were observed by XRD for the Cherokee Shale experiments (Table 1).

	Batch experiment Geochemistry														
	Depth(m)	Duration of Exposure		pH	Na/Cl	Ca	Mg	K	Na	Fe	Fe2	HCO3-	Cl-	SO4	Br
Cherokee Shale	1276	Prior		6.9	0.5	60.9	22.3	6.3	804.6	**	0.1	6.2	1015.5	9.5	2.3
		30 days	Biotic	5.9	0.6	83.0	25.0	7.4	910.8			46.1	1013.4	8.8	0.8
			Abiotic	5.9	0.6	83.0	25.1	7.3	923.5	0.0	0.0	44.9	987.9	9.1	0.9
		14 days	Biotic	6.3	0.5	77.7	23.7	6.9	863.9			43.4	1036.4	8.8	1.6
			Abiotic	6.1	0.5	75.9	23.0	6.9	834.2			43.9	1051.5	9.0	1.6
Chattanooga Shale	1276	Prior		6.9	0.5	60.9	22.3	6.3	804.6	**	0.1	6.2	1015.5	9.5	2.3
		30 days	Biotic	5.3	0.6	67.2	28.8	7.1	890.8	0.1	0.0	25.4	984.6	9.0	0.8
			Abiotic	5.3	0.6	63.1	27.4	6.3	841.8	0.3	0.1	26.0	948.1	9.0	1.0
		14 days	Biotic	5.5	0.5	63.9	26.9	7.1	862.1	0.1	0.0	21.6	1067.7	9.7	1.5
			Abiotic	5.6	0.5	63.1	26.6	7.2	856.4	0.1	0.0	21.0	1010.4	9.3	1.6
Pyrite	1321	Prior		7.1	0.5	70.2	24.7	6.5	758.0	**	0.1	6.6	930.9	16.7	1.6
		15 days	Biotic	3.7	0.6	61.6	26.6	6.5	802.1	0.0	6.6	pH too low	931.8	22.4	1.6
			Abiotic	3.9	0.5	60.7	26.7	6.4	805.4	0.0	6.5	pH too low	968.5	23.0	1.2
Dolomite	1321	Prior		7.1	0.5	70.2	24.7	6.5	758.0	**	0.1	6.6	930.9	16.7	1.6
		15 days		6.0	0.6	80.6	30.7	6.9	866.4	0.0	0.0	35.2	987.8	14.1	1.3
				6.0	0.5	77.3	28.6	6.5	804.6	0.0	0.0	34.5	986.6	14.6	1.1
* All units are presented as mmol/L															
** Was not detectable after 100x dilution															

Table 4.3. Table showing the changes in brine chemistry for each batch experiment after exposure to 100% pCO_2.

Chattanooga Shale

The Chattanooga shale is typically a silty, pyritiferous, black to dark-gray shale (Merriam, 1963). The 45-day experiment used an atypical sample of Chattanooga Shale that did not contain pyrite but contained gypsum, chlorite, mica, quartz and dolomite from a depth of 4065' from KGS 1-32 core. Because the Chattanooga Shale was so thin in the KGS 1-32 core, samples of Chattanooga Shale were collected from a nearby well (< 10 miles), drilled by Crest Petroleum (Peasal #1 well: API # 15-191-20169). This sample, collected from a depth of 4088' a few miles from Wellington oil field, did contain pyrite, chlorite, mica, quartz but did not contain gypsum or dolomite.

Unlike the experiments with Cherokee Shale mentioned above, the changes in brine chemistry observed after 14 and 30 day long exposure of the Chattanooga shale to 100% pCO_2 were less pronounced and were more variable between biotic and abiotic experiments (Fig 4.2). pH decreased from 6.9 to an average of 5.3 after 14 days exposure and 5.6 after 30 days exposure (Fig. 4.2). Bicarbonate decreased to an average of 25.6 mmol L^{-1} after 14 days exposure and 21.3 mmol L^{-1} after 30 days exposure. Notable increases in magnesium were also observed (Table 3). Magnesium increased from 22.3 mmol $L^{-}1$ 28.0 mmol L^{-1} after 30 days and 26.8 mmol L^{-1} after 14 days.

In contrast to the Cherokee experiments, several mineralogical changes occurred when powdered Chattanooga Shale was exposed to CO_2. Gypsum was detected after exposure to supercritical CO_2 in these experiments (Table 4).

$$CO_{2\,(aq)} + H_2O \longrightarrow H_2CO_3 \qquad \text{(Equation 4.1)}$$

$$H_2CO_3 + CaCO_3\,(s) \longrightarrow Ca^{2+}_{(aq)} + 2HCO_{3(aq)} \qquad \text{(Equation 4.2)}$$

$$FeS_2(s) + H_2CO_3 + \longrightarrow 2H_2S + CO_{3(aq)} + Fe^{2+}_{(aq)} \qquad \text{(Equation 4.3)}$$

pH dropped an average of 1.6 units in the Chattanooga experiments, likely due to absence of carbonate minerals in the Chattanooga experiments. In contrast, magnesium concentrations increased more in the brine after reaction with the Chattanooga Shale than the Cherokee shale and even more than pyrite. Concentrations of calcium increased greater the Cherokee shale experiments and calcium decreased in the pyrite experiment. The calcium was lower in the experiments that precipitated gypsum. The sulfate was probably still very high in the pyrite experiment because a large amount of pyrite was dissolved and did not precipitate all of the sulfate into gypsum. There is not a consistent or statistically relevant difference between the biotic and abiotic experiments. This may be due to low biomass concentrations in the reservoir or a lack of equilibrium in the system.

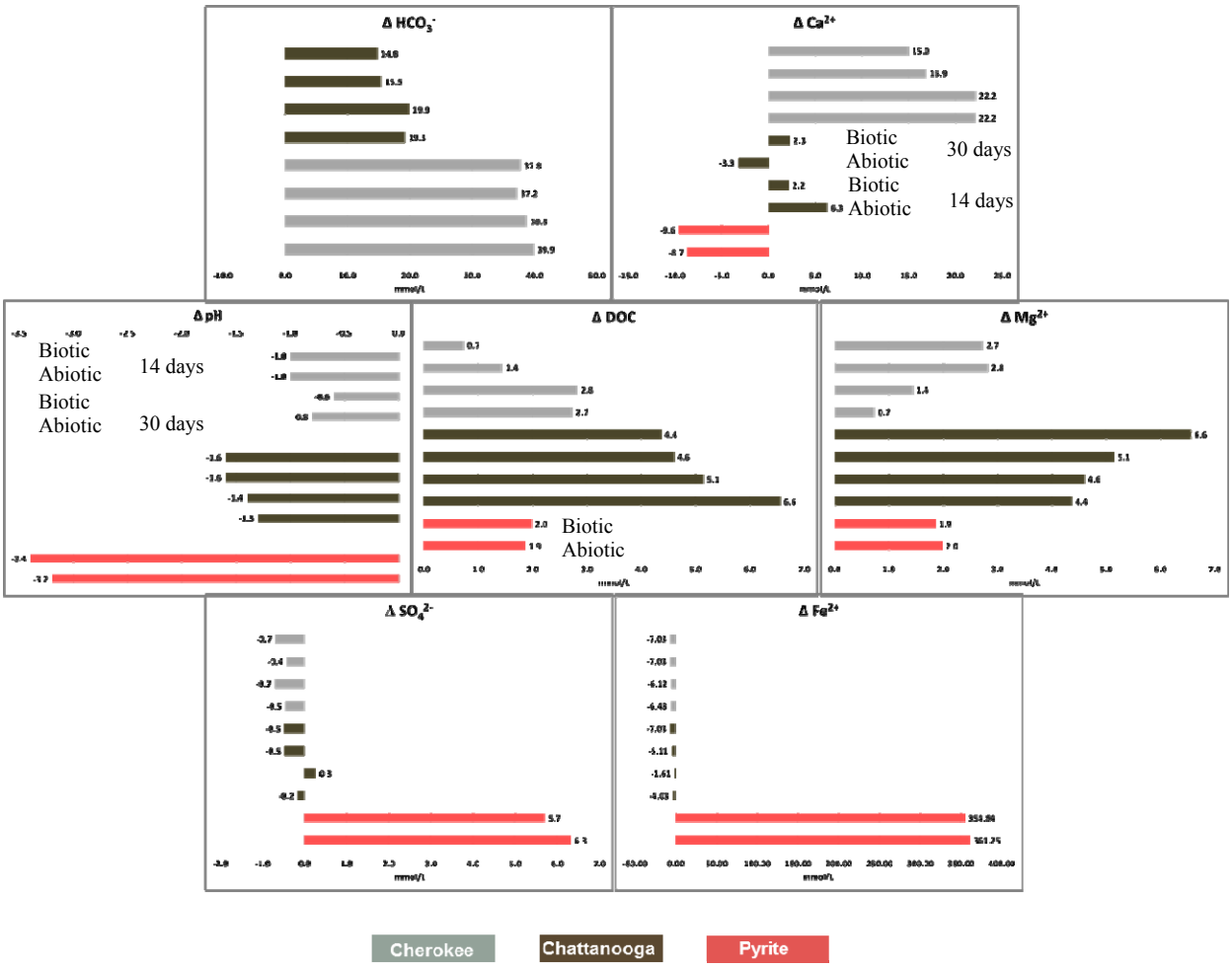

Figure 4.2. Changes in brine chemistry after CO_2 exposure with Cherokee Shale, Chattanooga Shale and Pyrite experiments. Shale experiments were conducted for 30 and 14 days and the pyrite experiment was conducted for 15 days.
.

Geochemical speciation was carried out using PhreeqC (Fig. 4.4 and Appendix Table D.2) and indicated that the brine used for the shale experiments (1276 m) was near or at equilibrium with all phases prior to CO_2 exposure but was just slightly under saturated with gypsum and anhydrite before exposure (Fig. 4.4 and Appendix Table D.2).

Chattanooga Shale

		Pyrite	Gypsum	Chlorite	Mica	Quartz	Dolomite
Before	4065'	X	✓	✓	✓	✓	✓
45 days	Biotic	X	✓	✓	✓	✓	✓
	Abiotic	X	✓	✓	✓	✓	✓
Before	4088'	✓	X	✓	✓	✓	X
30 days	Biotic	✓	✓	✓	✓	✓	X
	Abiotic	✓	✓	✓	✓	✓	X
15 days	Biotic	✓	✓	✓	✓	✓	X
	Abiotic	✓	✓	✓	✓	✓	X
7 days	Biotic	✓	✓	✓	✓	✓	X
	Abiotic	✓	✓	✓	✓	✓	X
5 days	Biotic	✓	✓	✓	✓	✓	X
	Abiotic	✓	✓	✓	✓	✓	X

Table 4.4: XRD Results of Chattanooga Shale exposed to supercritical CO_2 for 15 days.

Pyrite

The changes in brine chemistry observed after 15 days of exposure of pyrite to 100% pCO_2 were very different then the results of the shale experiments discussed above (Fig. 4.2). pH decreased sharply from 7.1 to 3.8. Reduced iron increased dramatically from 0.1 mmol L^{-1} to 6.6 mmol L^{-1}. Magnesium concentration increased from 24.7 to mmol L^{-1} 26.7 mmol L^{-1} after 15 days exposure (Fig 4.2). Sodium increased from 758 mmol L^{-1} to an average of 803.8 mmol L^{-1} after 15 days exposure. Calcium decreased from 70.2 mmol $L^{-}1$ 61.0 mmol L^{-1} after 15 days exposure and sulfate increased from 16.7 mmol $L^{-}1$ to 22.7 after 15 days. The most notable difference between this and the shale experiments is the increase in sulfate increase in the brine compared with the decreased observed the shale experiments.

Similar mineralogical changes to the Chattanooga Shale experiments were observed after exposure of pyrite alone (Table 2). Pyrite and rhomboclase (hydrated iron sulfate) which is a common alteration product of pyrite, were detected via XRD in the "before" sample of pyrite along with trace amounts of mica. Both experiments, biotic and abiotic, resulted in the removal

of the rhomboclase phase and the production of gypsum (Table 4.2). The rhomboclase is a potential source of the sulfate in the produced gypsum and the calcium could be coming from the aqueous phase. The produced gypsum was observable under the Scanning Electron Microscope (SEM) in the products of both the abiotic and biotic experiments (Fig. 4.3).

Pyrite – 15 days

	Mica	Gypsum	Anhydrite	Pyrite	Rhomboclase
Before	✓	X	X	✓	✓
Biotic	✓	✓	✓	✓	X
Abiotic	X	✓	✓	✓	X

Table 4.5: Bulk changes in mineralogy of powdered pyrite detected with XRD after 15-days of exposure to supercritical CO_2 at reservoir temperatures and pressures.

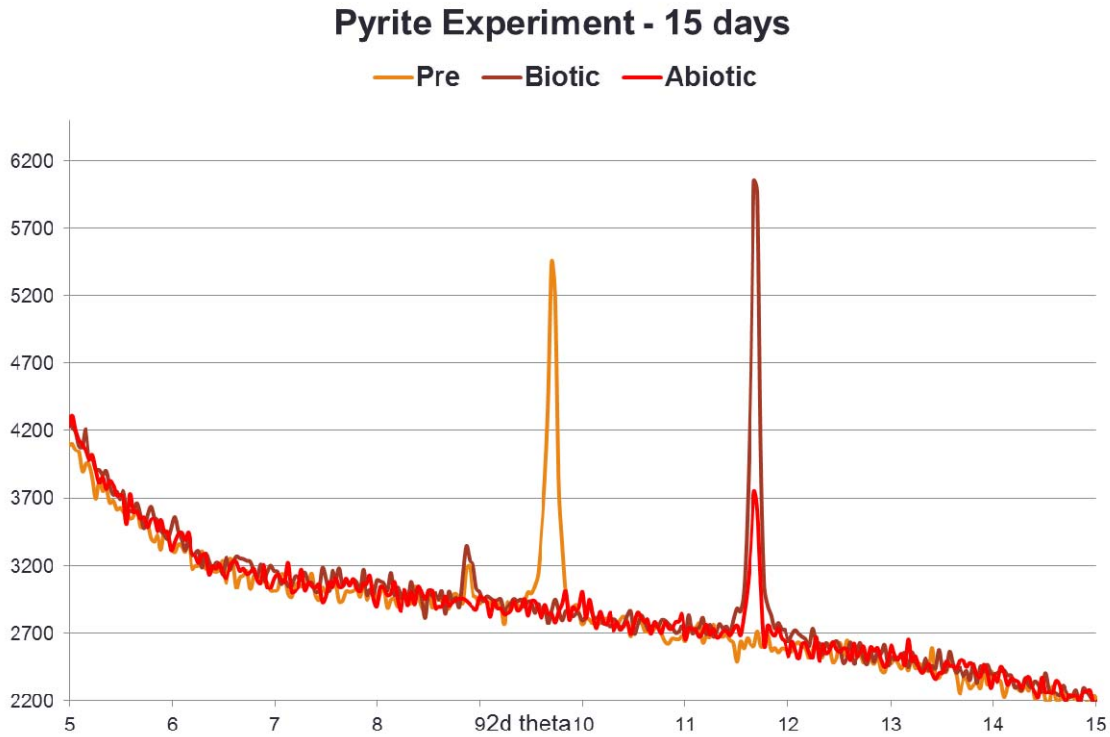

Figure 4.3. Overlay of XRD spectra of three powdered pyrite samples including the "pre" sample, and the products of both the biotic and abiotic experiments showing the bulk changes in mineralogy after 15-days of exposure to supercritical CO_2 with and without the presence of native microbial consortia at reservoir temperatures and pressures.

Scanning electron microscopy (SEM) was used to verify the XRD results, which indicated there was no gypsum or anhydrite present in the "pre" samples but was precipitated

during the pyrite and Chattanooga Shale experiments. Gypsum crystals were identified in reacted samples but were not located within the "pre" samples (Fig. 4.3).

In summary, there was much larger decreases in pH and reduced iron, and a *decrease* in calcium in the pyrite experiments compared to the shale experiments. The less pronounced pH drop in the Cherokee experiments can likely be attributed to the presence of dolomite and calcite in the Cherokee samples. Overall, the brine of the Cherokee Shale experiments show greater change after CO_2 exposure. This is reflective of the XRD results, which indicate that the Chattanooga Shale had precipitation of secondary minerals after CO_2 exposure, whereas the Cherokee Shale did not.

Mineral Saturation States

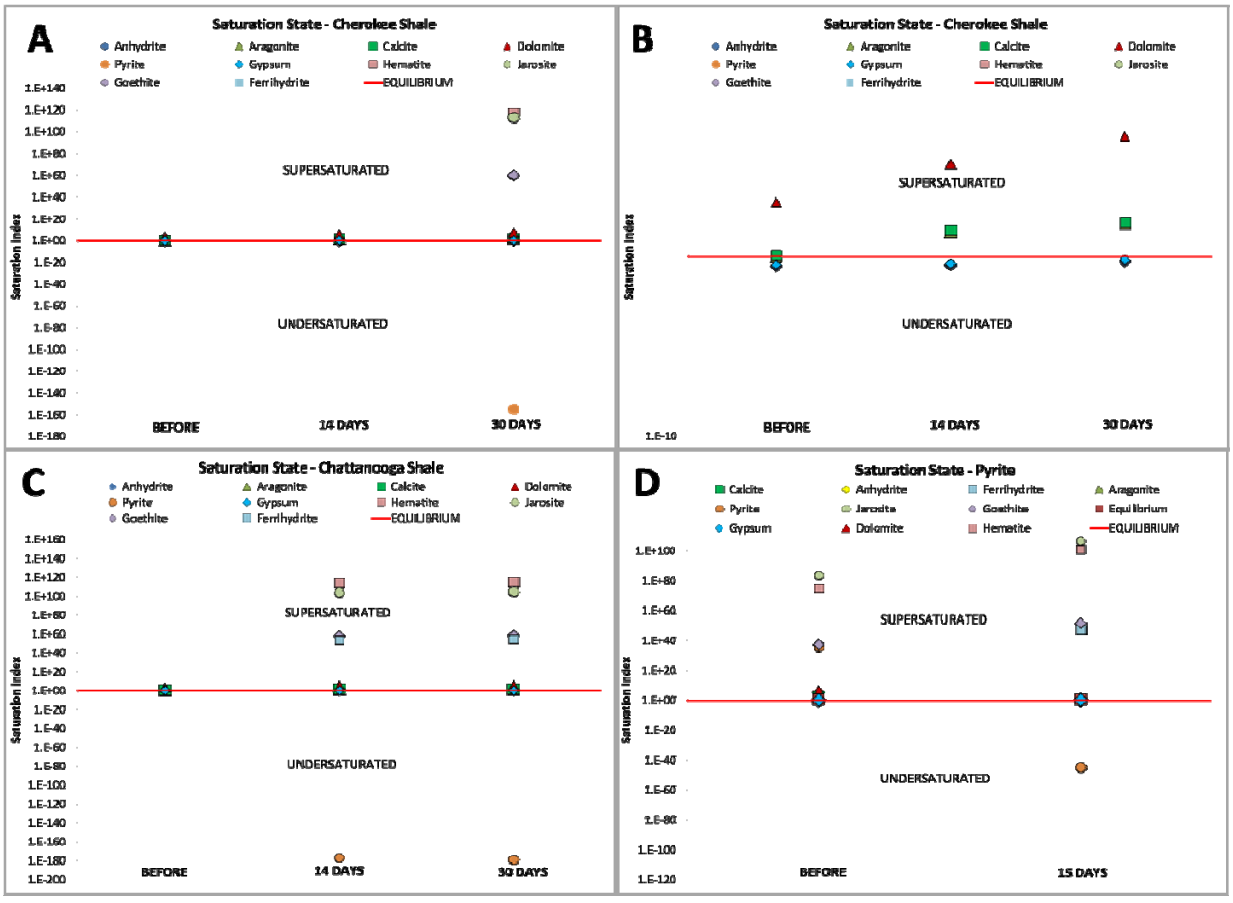

Figure 4.4. Results of geochemical speciation carried out for the Cherokee Shale experiments using PhreeqC showing that the brine (1276 m) was near equilibrium with all phases prior to CO_2 exposure but moved further out of equilibrium with phases with experiment duration (A). Zooming in on the values shows that although the brine was near equilibrium with all phases prior to CO_2 exposure, and it was slightly under saturated with gypsum and anhydrite before exposure (B). Results of geochemical speciation carried out for the Chattanooga Shale experiments show that the brine (1276 m) was near equilibrium with all phases prior to CO_2 exposure and became oversaturated with hematite, jarosite, goethite, and ferrihydrite after 14 and 30 days of CO_2 exposure and the brine (C). Results of geochemical speciation carried out for the pyrite experiments show that the brine (3121 m) was out of equilibrium with several mineral phases before the start of experiments and became even more oversaturated with hematite, jarosite, goethite, and ferrihydrite after 14 and 30 days of CO_2 and became undersaturated with pyrite after 15 days of CO_2 exposure.

PhreeqC indicated that the brine used for the pyrite experiment (4335') was supersaturated with jarosite, hematite, goethite, and pyrite. Speciation of pyrite experiments after 15 days show that the brine became under saturated with pyrite after CO_2 exposure and over saturated with ferrihydrite (Fig. 4.9).

Microbiology

The raw water was stored in the refrigerator for between 8-12 months before being used in these experiments. Quant-iT™ PicoGreen® dsDNA can detect and quantify small amounts of DNA and was used to quantify the microbial population present in the brine before and after exposure to 100% pCO_2. Quant-iT™ PicoGreen® dsDNA reagent is an ultra-sensitive fluorescent nucleic acid stain for quantitating double-stranded DNA (dsDNA) in solution (www.invitrogen.com). The DNA concentrations in the "pre" samples changed significantly since initial sampling. DNA concentrations were measured in 4335' and 4118' immediately after sampling and indicated there were 550 cells ml^{-1} and 450 cells ml^{-1} of sample respectively. In contrast, the refrigerated raw brine from 4335' and 4118' had 10,000 and 410,000 cells ml^{-1}. Pico green gives results in ngL^{-1} which was converted using $6.02x10^{17}$ daltons ug^{-1}, 660 daltons per base pair, and 6 million base pairs per cell (average for *Pseudomonas*). This suggests the raw brine underwent substantial growth during storage. The brine was analyzed with PicoGreen again after each experiment but detected only negligible amounts of DNA after exposure to

100% pCO_2 after every experiment, including after only 5 days. These results indicate that the entire microbial community was obliterated with exposure to 100% pCO_2.

Biomass concentrations cells/ml		
	1276 m Brine	**1321 m Brine**
"Pre"	450	550
After refrigeration	410.000	10,000
Post 14 day exposure w/ Cherokee	0	0
Post 14 day exposure w/ Chattanooga	0	0
Post 30 day exposure w/ Cherokee	0	0
Post 30 day exposure w/ Chattanooga	0	0
Post 15 day exposure w/ pyrite	0	0

Table 4.6. Table showing starting biomass concentrations in brine from 1276 m and 1321 m and how biomass concentrations in the brine changed after prolonged refrigeration and exposure to supercritical CO_2 in batch experiments.

These results suggest that the vast majority of organisms near the wellbore will be lysed resulting in the release of organic carbon. A report by Morozova et al. (2010) examined the effects of CO_2 injection on microbial community in a deep saline aquifer and reported that after injection with CO_2, a shift in community structure occurred, with methanogens outcompeting sulfate reducers after ~1-2 months but eventually reestablishing after a 5-month lag period. This was probably due to initial lysing of the SRB and the survival of methanogens (likely due to their ability to tolerate lower pH) and subsequent adjustment of SRB. This study supports that a release of DOC will follow behind plume migration of at least the most concentrated portion of the CO_2 plume.

Conclusions & Implications

Gypsum precipitation occurred when the Chattanooga Shale containing pyrite was exposed to 100% pCO_2. Similarly, gypsum precipitation and rhomboclase dissolution occurred when pyrite was exposed to 100% pCO_2. This suggests the pyrite in the Chattanooga was responsible for the gypsum precipitation. Although XRD did not detect bulk mineralogic changes in Cherokee Shale experiments, decreases in iron, increases in magnesium, and decreases in calcium indicate reactions with the Cherokee Shale *are* occurring. These reactions,

however, may occur at a slower rate in the Cherokee Shale and may manifest as detectable changes in mineralogy after longer periods of exposure. The more pronounced changes to the brine chemistry in the Cherokee Shale experiments are likely due to substantial dissolution of minerals without secondary mineral precipitation in Cherokee experiments. These results have serious implications for carbon sequestration. Precipitation and dissolution will impact reservoir porosity and permeability. Our results indicate that precipitation of secondary gypsum will occur when Arbuckle rocks containing pyrite are exposed to CO_2. This could either beneficially fill pore space and fractures in seals resulting in even better sealing of the reservoir or it could detrimentally clog valuable pore space in the CO_2 storage reservoir, lowing storage capacity, or decreasing injection capability.

References Cited

Dixon, N. M. and Kell, D. B., (1989). The inhibition by CO_2 of the growth and metabolism of microorganisms. Journal of Applied Bacteriology 67, 2: 109-136.

Emberley, S., (2004). Geochemical monitoring of fluid-rock interaction and CO_2 storage at the Weyburn CO_2-injection enhanced oil recovery site, Saskatchewan, Canada. Energy. 29, 9-10: 1393-1401.

Kaszuba, J. P., Janecky, D. R., (2005). Experimental evaluation of mixed fluid reactions between supercritical carbon dioxide and NaCl brine: Relevance to the integrity of a geologic carbon repository. Chemical Geology. 217, 3-4: 277-293.

Kaszuba, J.P., Janecky, D.R. and Snow, M.G., (2004). Experimental evaluation of mixed fluid reactions between supercritical carbon dioxide and NaCl brine: Relevance to the integrity of a geologic carbon repository. Chemical Geology. 217, 3-4: 277-293.

Kharaka, Y. K., Thordsen, J. J., (2009). Potential environmental issues of CO_2 storage in deep saline aquifers: Geochemical results from the Frio-I Brine Pilot test, Texas, USA. Applied Geochemistry 24, 6: 1106-1112.

Lu, P., (2011). Navajo Sandstone-brine-CO_2 interaction: implications for geological carbon sequestration. Environmental Earth Sciences. 62, 1: 101-118.

Merriam, D. (1963). The Geologic History of Kansas. Kansas Geological Survey Bulletin: 317.

Parkhurst, D. L. (1995). User's guide to PHREEQC : a computer program for speciation, reaction-path, advective-transport, and inverse geochemical calculations. Water-resources investigations report ; 95-4227, 143: 129.

Weishaar, J. L., Aiken, G. R., (2003). Evaluation of Specific Ultraviolet Absorbance as an Indicator of the Chemical Composition and Reactivity of Dissolved Organic Carbon. Environmental Science & Technology. 37, 20: 4702-4708.

Wigand, M., (2008). Geochemical effects of CO_2 sequestration in sandstones under simulated in situ conditions of deep saline aquifers. Applied Geochemistry. 23, 9: 2735-2745.

CHAPTER 5

Conclusions and Implications

This study presents strong evidence of hydraulic separation of the Upper and Lower Arbuckle and uncovered some mutually beneficial evidence of a stratigraphically bound fracture-vug system evidenced by basically homogeneous brines in the Lower Arbuckle. The tight, dense, lowly permeable zone with high impedance is limited hydraulic connectivity of the Upper and Lower Arbuckle which suggest it may serve as an important impediment the buoyant behavior and a CO_2 plume, which will increase pore space and solubility trapping. The presence of this baffle is essential because the data also show that the Lower Arbuckle brines are relatively homogenous and undergoing rapid mixing due to the fracture-vug system suggesting the plume will travel relatively quickly to the central baffle. The data suggest there will be limited vertical communication with the lower Arbuckle due to relatively short vertical fractures closely linked to vuggy carbonate layers including intra-formational breccias developed along small disconformities in the lower Arbuckle.

The work mentioned above was complemented by a series of batch experiments, which also produced data with conflicting implications for carbon sequestration potential in Kansas, regarding injectivity and caprock integrity. The precipitation of gypsum caused by the presence of pyrite in the reservoir will positively impact the seal integrity by beneficially filling pore space or fractures in seals resulting in even better sealing of the reservoir but could the same reactions could detrimentally clog valuable pore space in the CO_2 storage reservoir, lowering storage capacity, or decreasing injection capability.

The results presented here are mostly encouraging for the prospect of carbon storage in the Arbuckle saline aquifer. Although significant CO_2 reactivity of the caprock materials was

observed, reactions with the primary seal (Chattanooga Shale) are beneficial to integrity. Dissolution, however, was the dominant processed observed when the secondary seal (Cherokee Shale) was exposed under the same conditions. The heterogeneity of the reservoir is beneficial for carbon sequestration and will encourage dissolution and solubility trapping. No evidence for direct leakage paths through the reservoir was observed. Finally, because of the highly fractured nature of the reservoir, the presence of the central baffle and proof of long-term hydraulic separation in the reservoir is vital to qualifying the Arbuckle aquifer as a competent carbon storage reservoir.

Acknowledgements

The research discussed in Chapter 4 of this thesis was supported by the U.S. Department of Energy (DOE) and was supported in part by an appointment to the National Energy Technology Laboratory Research Participation Program, sponsored by the U.S. Department of Energy and administered by the Oak Ridge Institute for Science and Education (ORISE).

APPENDIX A

Supporting information

Source	Depth Interval	Average depth	Interval thickness	Formation
DST 1	3664'-3690'	3677'	26'	Mississippian
DST 4	4175'-4190'	4182.5'	15'	Arbuckle
DST 3	4280'-4390'	4335'	110'	Arbuckle
SWAB 4	4366'-4380'	4373'	14'	Arbuckle
DST 2	4465'-4575'	4520'	110'	Arbuckle
SWAB 3	4872'-4878'	4875'	6'	Arbuckle
DST 8	4866'-4885'	4875.5'	19'	Arbuckle
DST 7	4917'-4937'	4927'	20'	Arbuckle
SWAB 2	4924'-4932'	4928'	8'	Arbuckle
SWAB 1	5000'-5020'	5010'	20'	Arbuckle
DST 6	5026'-5047'	5036.5'	21'	Arbuckle
DST 5	5133'-5250'	5191.5'	117'	Granite basement

Table A.1. Brine sample summary showing the sampling method, depth interval, average depth, sampled interval thickness and rock formation sampled.

16s rRNA Bacterial Primers	8 forward primer 5'-AGAGTTTGATCMTGGCTCAG-3' with the 519 reverse primer 5'-GTATTACCGCGGCTGCTGG-3'
	338 forward primer 5'-ACTCCTACGGGAGGCAGC-3' with the 907 reverse primer 5'-CCGTCAATTCMTTTRAGTTT-3'.
16s rRNA Archaeal Primers	344 forward primer 5'-ACGGGGCGCAGCAGGCGCGGA-3' with the 915 reverse primer 5'-GTGCTCCCCCGCCAATTCCT-3'.
qPCR Primers	1369 forward primer 5'-CGGTGAATACGTTCYCGG-3' with the 1492 reverse primer 5'-GGWTACCTTGTTACGACTT-3' and the TAMRA 6 FAM 1389 forward probe CTTGTACACACCGCCCGTC.

Table A.2: Bacterial and Archaeal primers used

Order	Species	Accession #	Isolation Location	4520'	4335'	4220'
Bacteriodales	Alkaliflexus imshenetskii	NR042317.1	Soda Lakes	--	1%	4%
	Cyclobacteriaceae bacterium MIM18	HM140980.1	Haloalkaline Lake	7%	11%	21%
	Marinilabiaceae bacterium AP1	GQ922444.1	Soda Lakes	6%	7%	3%
Firmicutes	Alkalibacter saccharofermentans	NR042834.1	Soda Lakes	--	3%	1%
Actinobacteria	Xylanimonas cellulosilytica DSM 15894	CP001821.1	Decaying Tree	5%	8%	3%
Proteobacteria	Halomonas sp. HB.br	GU228481.1	Organic waste reactor	55%	17%	45%
	Halomonas nitritophilus	GU113002.1	Mud Volcano	--	--	3%

Table A.3. Summary of bacteria sequenced from the Arbuckle saline aquifer in KGS 1-32 in Wellington oil field in Sumner County, Kansas.

APPENDIX B

CORE-FLOOD EXPERIMENTS

Core-flood experiments were conducted at the Geomechanics and Coreflow laboratory at the National Energy and Technology Laboratory in Pittsburgh, Pennsylvania. (http://www.netl.doe.gov/onsite_research/Facilities/seq_core.html) using the CFS-839Z flow-through system (CoreTest Systems, Inc.). The instrument was wiped with ethanol and flushed with 10% bleach solution through all the inlet and outlet tubing prior to each run. 100 ml of brine was flushed through the instrument before mixing with CO_2 to fill the dead space of all the tubing. The accumulator vessels were heated to 40°C for three hours prior to mixing CO_2 with brine because the density of supercritical CO_2 is extremely sensitive to temperature and pressure variations. The accumulator was pressured to 2000 psi before introducing CO_2 to the brine to assure the correct density of CO_2 was achieved. Time of sampling was recorded once brine breakthrough was observed at the sampling port. Samples were collected for cations, anions, and pH. A flow rate of 0.5 ml/min was set on the instrument to mimic the reported flow rates of the Arbuckle aquifer. However, this rate was not achieved during the first experiment due to a problem with the back pressure regulator (BPR) on the instrument but was achieved for all subsequent experiments. Samples were collected continuously throughout the experiment, initially every fifteen minutes until pH stabilized somewhat or I needed to sleep, whichever came first. Then sampling occurred once an hour. Table B.1 shows the depth of the fractured caprock used, if the brine used was biotic or abiotic, the pore and confining pressures applied, the concentration of the CO_2 in brine, the total volume run through the sample, the brine used, and the flow rate and duration of each of the four core-flood experiments conducted.

CF#	Fractured rock sample	Depth (m)	Biotic/ Abiotic	Pore Pressure (psi)	Confining Pressure (psi)	[CO_2] Mol/kg	Duration (hours)	CO_2/Brine Volume (ml)	Brine (m)	Flow rate ml/min
1	Chattanooga	1239.0	Biotic	2000	2300	0.2	24	2000	1527	1.5
2	Chattanooga	1238.9	Abiotic	2000	2300	0.2	47	1612	1527	0.5
3	Cherokee	1079.5	Biotic	2000	2300	0.2	38	1222	1527	0.5
4	Cherokee	1079.49	Abiotic	2000	2300	0.2	36	1075	1527	0.5

Table B. 1. Core-flood parameters used for each of the 4 core-flood experiments conducted at NETL.

Figure B. 1. Images of fractured core plugs used in core-flood experiments. Samples were fractured by by Hema J. Siriwardane of the Civil and Environmental Engineering at West Virginia University. Samples were then reassembled and epoxied along the outer surface to hold the sample together.

Core plug dimensions			
Fractured rock sample	Depth (m)	L (mm)	D (mm)
Chattanooga	1239.0	70.11	39.20
Chattanooga	1238.9	75.37	39.15
Cherokee	1079.5	65.10	38.13
Cherokee	1079.49	23.54	38.70

Table B. 2. Core plug dimensions for each of the core plugs used in the 4 core-flood experiments conducted at NETL.

Core plug samples were prepped according to the guidelines outlined in the CFS-839Z flow-through system (CoreTest Systems, Inc.) manual. The sample was first wrapped with a single layer of Teflon tape. The sample was then wrapped with a single layer of aluminum foil. A sleeve of heat-shrink Teflon was cut to cover the entire sample and the core holder assembly, including the o-rings (Figure B.2) which was then shrunk using a heat gun until a good seal was

achieved. However, this configuration rarely worked properly and it seems the acidified brine continued to pass around the sample rather than through the core plug fracture as was desired.

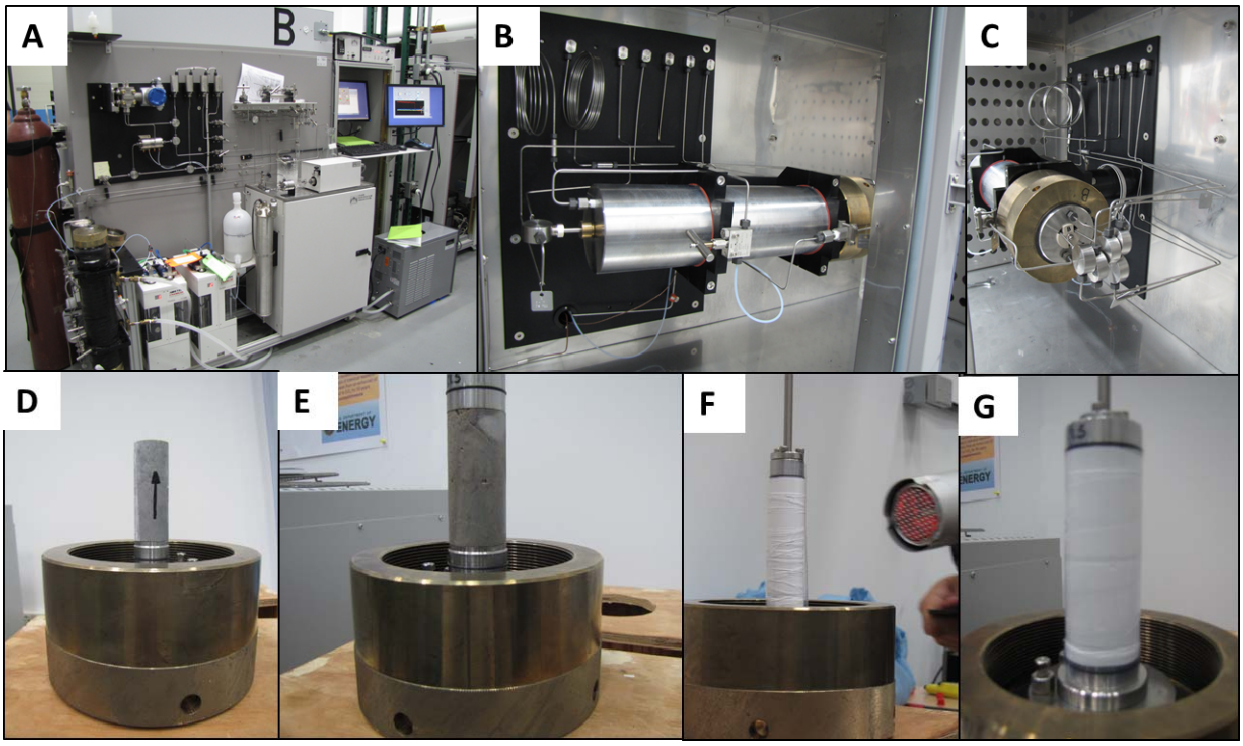

Figure B. 2. Images of CFS-839Z flow-through system and core plug preparation. Panel A shows the control side of the CFS-839Z flow-through system including the dip-tube CO_2 tank, CO_2 and brine accumulators, pumps, back pressure regulators, pore pressure and confining pressure controls, accumulator chiller unit and computer system which is all mounted to the back of the oven. Panel B shows the Hassler cell inside the oven which the core plug is loaded into with inlet and outlet tubing. Panel C shows the end of the Hassler cell with inlet tubing for both the confining and pore pressure of the cell. Panel D shows the first step in preparing the core plug for an experiment. Panel E shows step 2. After the core plug is placed between the holders it is wrapped with Teflon tape, aluminum foil and another layer of Teflon tape. Heat shrink Teflon is then placed over the wrapped core plug and shrunken using a heat gun. Panel F shows the heat fun shrinking this tape on a 1" core plug. Panel G shows a sample ready to be placed into the Hassler cell in the oven.

Between each experiment the back pressure regulator was rebuilt and filled with oil. Any o-rings that are exposed to CO_2 were be replaced due to the structural damage exposure to CO_2 causes by carbonation of the materials including accumulators and BPRs. The previous core plug was removed and the ends trimmed off for SEM. All tubing and accumulators of the instrument was flushed with 10% bleach solution and then flushed twice with deionized water

and leak checked. The next sample was then prepared. Sampling bottles were also prepared and labeled.

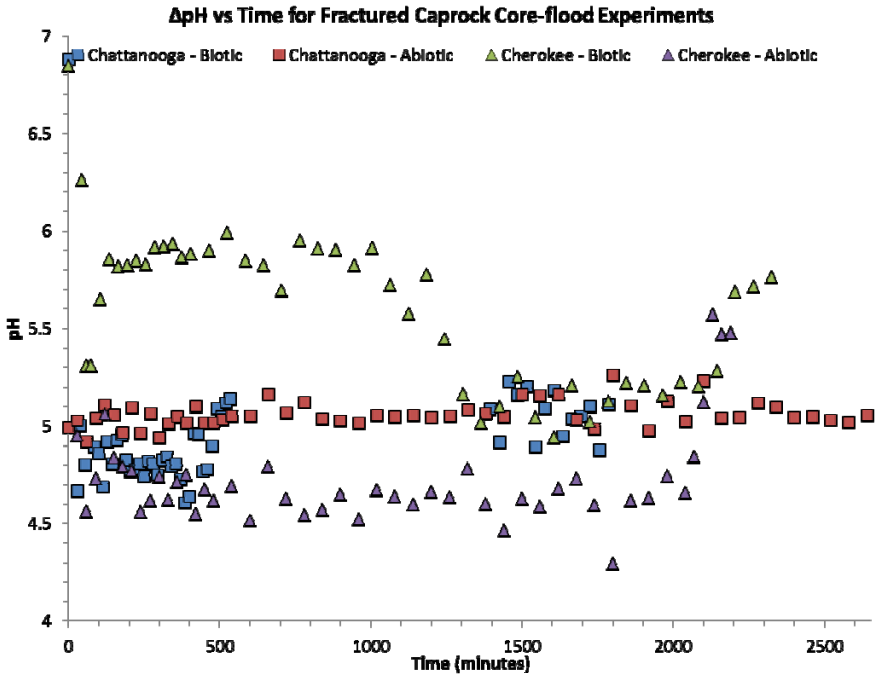

Figure B. 3. Changes in pH during each core-flood experiment. Missing data points indicate a disruption in the experiment and hiatus in sampling (caused by problems with the back pressure regulator) and each experiment had different lengths of duration depending on volume of brine used.

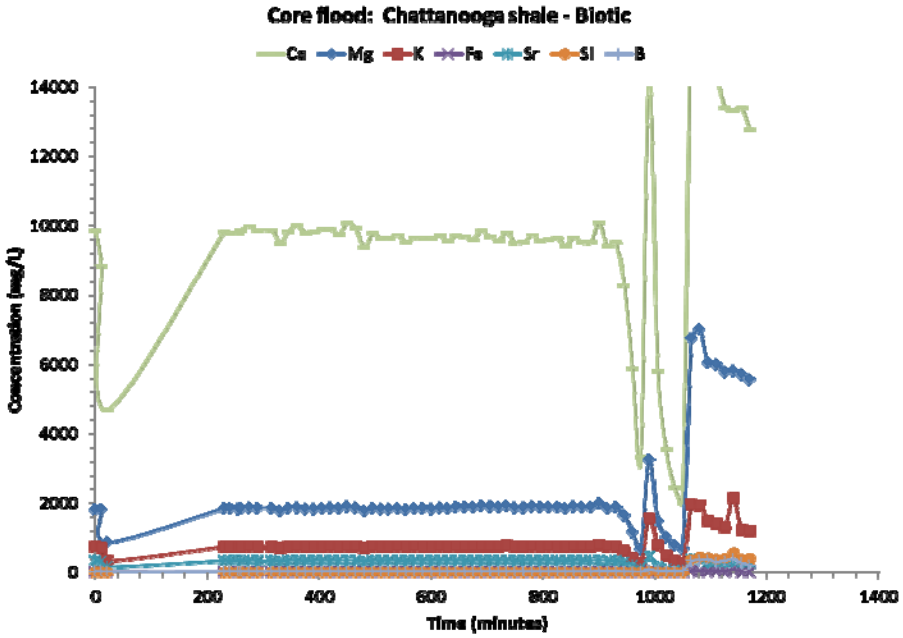

Figure B. 4. Cation and anion results of the core-flood experiment with a Chattanooga Shale sample and CO_2 acidified biotic brine. This was the first experiment conducted and had the most complications. The experiment had to be stopped

at 480 minutes for several hours but it does not appear to have affected the results. These results suggest the acidified brine may have bypassed the fracture travelled between the Teflon tape and heat shrink Teflon. Around 1000 minutes a pH increase was observed and a leak was found. The leak was fixed by tightening a fitting but pH never really dropped. Pressured were bouncing around during this time.

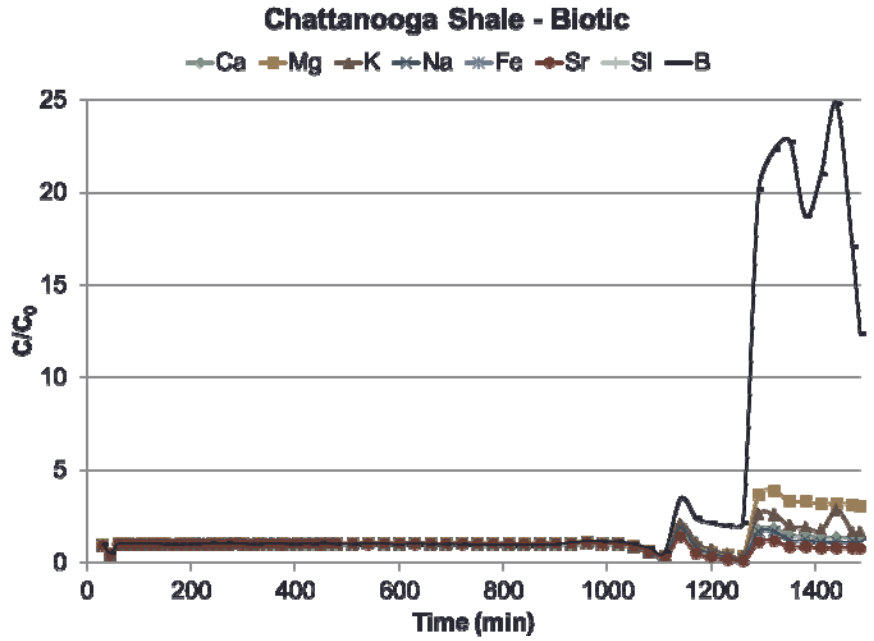

Figure B. 5. C/Co for cation and anion results of the core-flood experiment with a Chattanooga Shale sample and CO_2 acidified biotic brine.

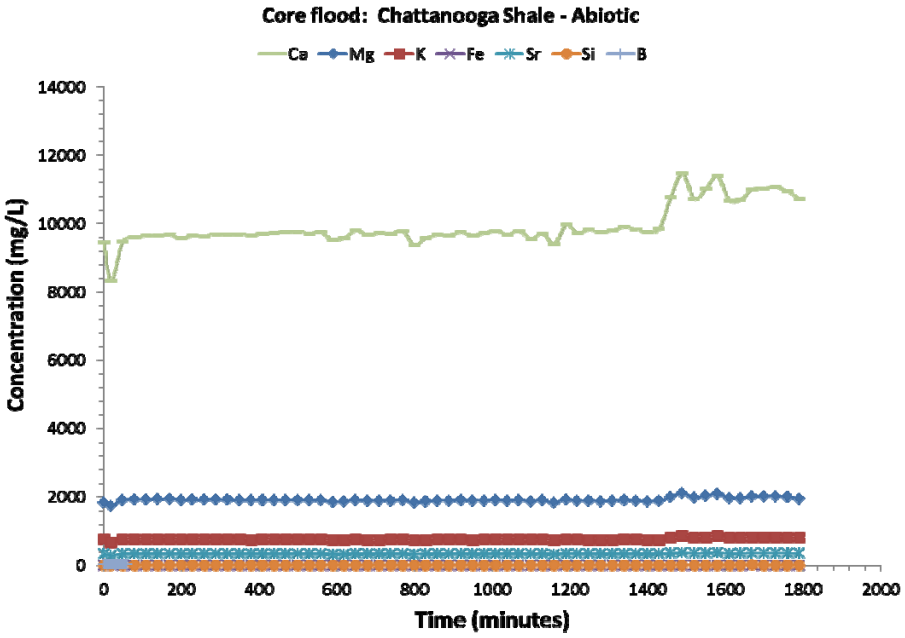

Figure B. 6. Cation and anion results of the core-flood experiment with a Chattanooga Shale sample and CO_2 acidified abiotic brine.

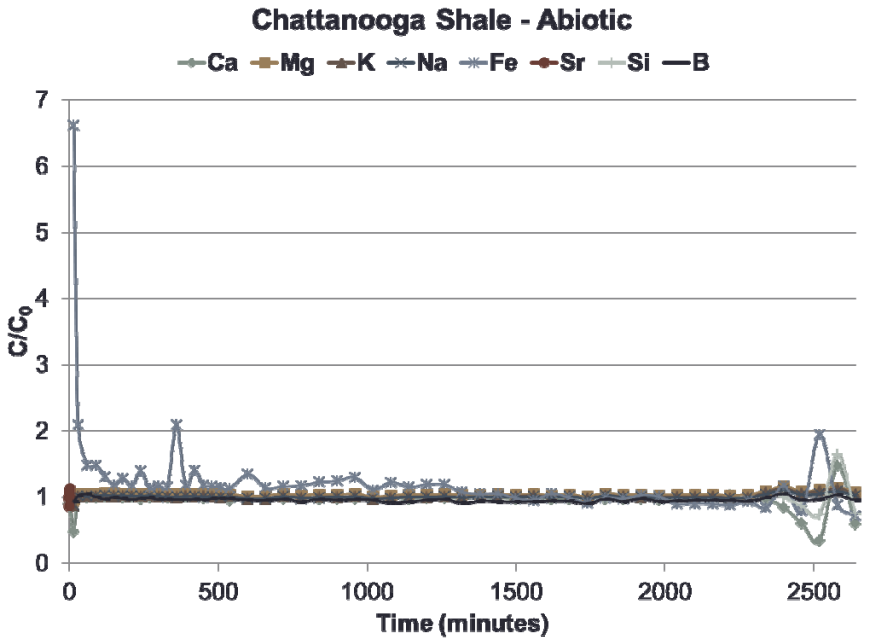

Figure B. 7. C/Co for cation and anion results of the core-flood experiment with a Chattanooga Shale sample and CO_2 acidified abiotic brine.

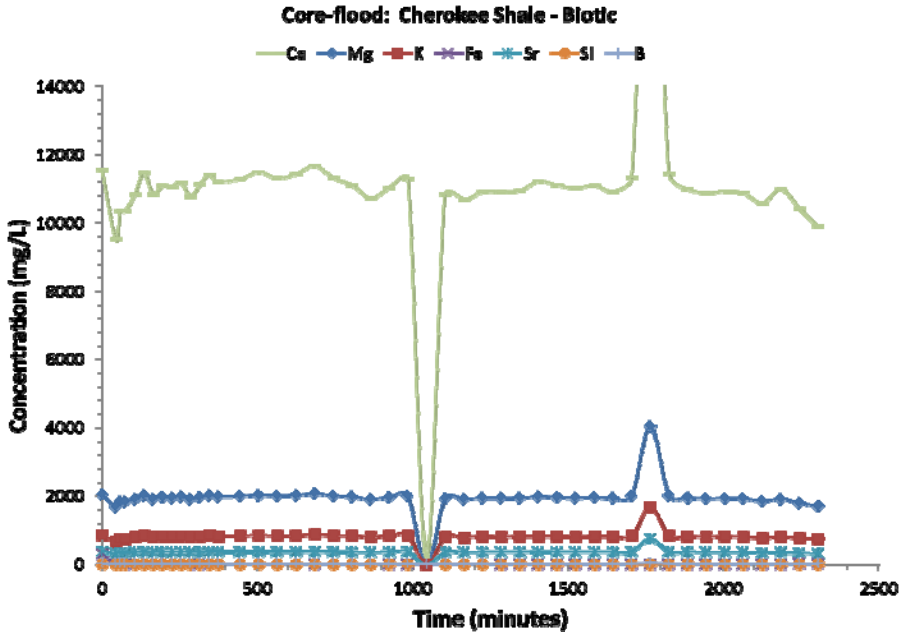

Figure B. 8. Cation and anion results of the core-flood experiment with a Cherokee Shale sample and CO_2 acidified biotic brine.

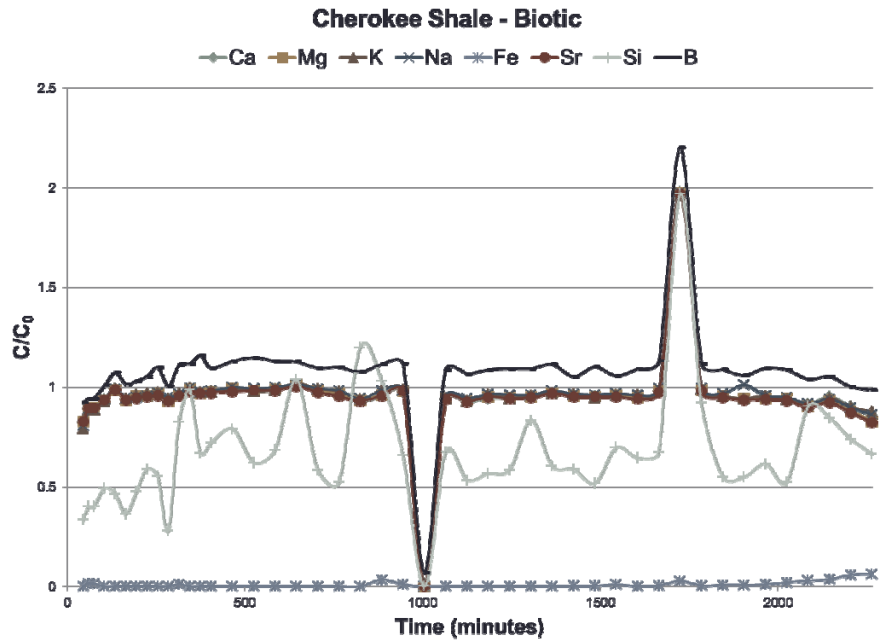

Figure B. 9. C/Co for cation and anion results of the core-flood experiment with a Cherokee Shale sample and CO_2 acidified biotic brine.

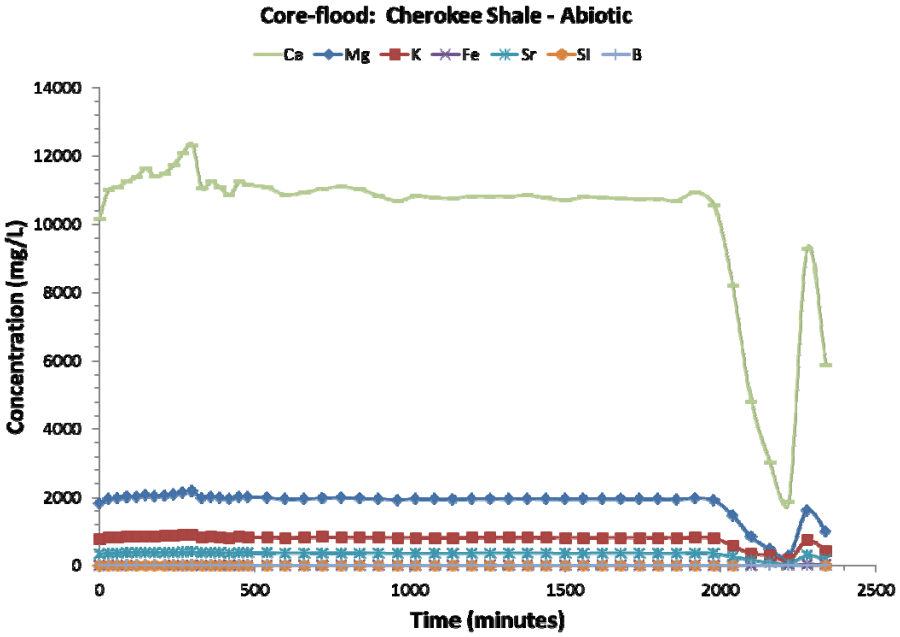

Figure B. 10. Cation and anion results of the core-flood experiment with a Cherokee Shale sample and CO_2 acidified abiotic brine.

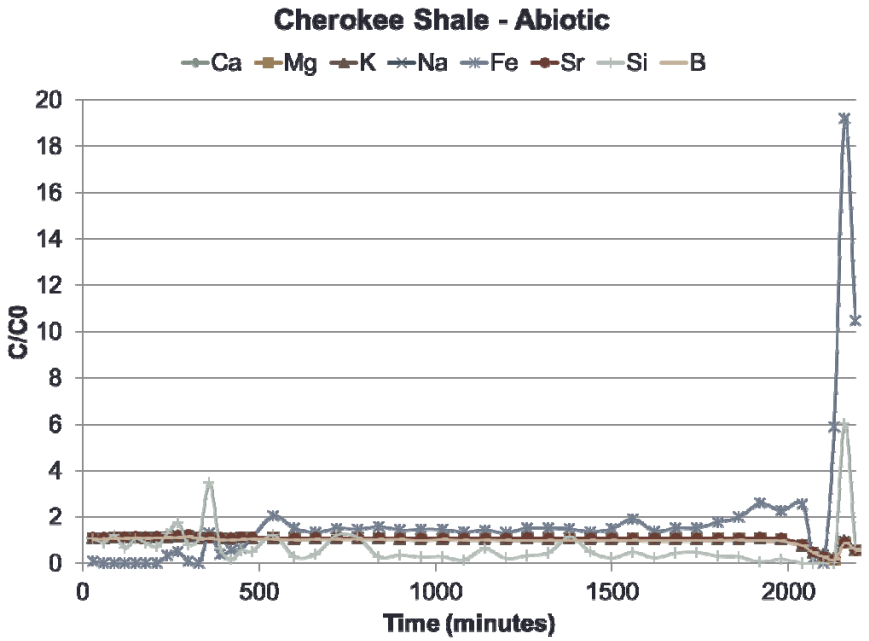

Figure B. 11. C/Co for cation and anion results of the core-flood experiment with a Cherokee Shale sample and CO_2 acidified abiotic brine.

APPENDIX C

For Cultivation of Heterotrophic Fermenters:

Suspend 28.4 g Schaedler's Broth in 1 L DIW, stir and boil 1 min until completely dissolved. Prepare anaerobically (does not require resazurin or cysteine). Autoclve 15 min, slow speed. To confirm the presence of heterotrophic fermenters after inoculation, check for visible growth in 1 week. Adjust PH to 7.2

For Cultivation of Denitrifiers:

Figure C.1. Media recipe for fermenting media used in MPN.

For Cultivation of Iron-Reducing Bacteria:

1.5071g sodium acetate
2.5 g NaHCO3
0.1 g CaCl2*2H2O
0.1 g KCl
1.5 g NH4Cl
1.0 g KH2PO4
0.1 g MgCl2*6H2O
0.0488 g MgSO4
9 mL trace metal solution
5 mL vitamin solution
200 mL 0.5 M Fe3+ ions

Prepare 0.5 M Fe3+ ions by making a 0.5 M FeCL3 solution in DIW, titrating to pH 7 using HCl and NaOH. Mix measured reagents in a media bottle, diluting to 1 L. Prepare anareobically (not using resazurin or cysteine). Autoclave 15 min using the slow cycle. After inoculation, aseptically pressurize the bottles using a 70:30 mix of H2:CO2 to 140 kPa (about ~10 s with a steady stream of gas bubbles). To confirm the presence of iron reducers, check growth after two months' incubation at room temperature. Prepare an anaerobic, sodium acetate solution by dissolving 35 g NaC2H3O2 in DIW and diluting to 100 mL. Additionally, anaerobically prepare a bipyridine solution by dissolving 0.5g bipyridine in DIW and diluting it to 250 mL. Inject these solutions into media potentially containing iron reducers in the following quantities(for testing 5 mL): 200uL bipyridine and 400uL sodium acetate solutions.

Figure C.2. Media recipe for iron-reducing media used in MPN.

For Cultivation of Sulfate-Reducing Bacteria

3.0 g Na_2SO_4
0.2 g KH_2PO_4
0.3 g NH_4Cl
0.5 g KCl
0.15 g $CaCl_2*2H_2O$
1.0 g NaCl
0.4 g $MgCl_2*6H_2O$
1.688 g sodium acetate
9.0 mL trace metal solution
4.0mL vitamin solution

Mix ingredients in a media bottle and dilute to 1 L with DIW. Prepare anaerobically (with both resazurin and cysteine). Autoclave 15 min at the slow setting. Just before use, add 0.1 mL of sterile, CO_2-saturated $NaHCO_3$ solution (84 g/L) to each serum bottle in an MPN dilution. After inoculation, aseptically pressurize the bottles with a 70:30 mix of H_2:CO_2 to 140kPa(purge ~10 s with a steady steam of gass bubbles). Sulfate reducing bacteria are dected with darkening of lead acetate paper.

Figure C.3. Media recipe for sulfate-reducing media used in MPN.

For the Cultivation of Methanogens:

0.75 g KH_2PO_4
0.89 g K_2HPO_4
0.36 g $MgCl_2*6H_2O$
0.9 g NH_4Cl
9.0 mL trace metal solution
3.0 mL vitamin solution
1.5071 g sodium acetate
2.5 g sodium formate

Mix ingredients in a media bottle and dilute to 1 L with DIW. Prepare anaerobically (with both resazurin and cysteine). Autoclave 15 min at the slow setting. Aseptically pressurize after inoculation with a 70:30 mix of H_2:CO_2 to 140 kPa (~10 s in a 10 mL Wheaton bottle with a steady stream of gass bubbles). Incubate at room temperature a minimum of 6 weeks, 2 months is preferred. Detection of methane in the head space via gas chromatography analysis confirms the presence of methanogens. Negative controls must be used to establish a background methane concentration.

Figure C.4. Media recipe for methanogenic media used in MPN.

APPENDIX D

Brine data

Depth (Ft)	T °c	pH (field)	HCO_3	DOC	CH_4	Br	Cl	N/NO_3	P/PO_4	SO_4
4188	43.9	7.1	6.2	12	7.E-01	1.1	969	0.07	8.42E-05	8.4
4335	46.0	6.9	6.6	11	7.E-01	0.9	889	0.09	1.05E-04	15.3
4370	**	6.7	4.0	**	**	1.2	1332	**	**	8.6
4520	50.3	6.4	4.2	1	6.E-02	1.5	1802	0.16	7.37E-05	9.5
4875	**	6.2	2.8	**	**	2.1	2873	**	**	3.8
4927	53.3	6.3	1.9	9	6.E-01	2.1	2646	0.25	6.84E-04	3.8
4928	**	6.2	2.6	**	**	2.3	2894	**	**	3.2
5010	**	5.7	1.6	14	**	2.8	3326	0.18	**	3.1
5037	54.4	6.0	1.1	19	9.E-01	2.7	3114	0.24	5.05E-04	2.8
5191	54.3	6.8	1.9	3	**	2.6	2507	0.32	1.05E-03	2.6

Depth (Ft)	Ca	K	Mg	Na	B	Si	Fe^{2+}	Fe total	Al	Sr
4188	61	6	22	805	12	0.1	0.4	0.2	0.1	3.7
4335	70	7	25	758	12	0.1	0.5	0.2	0.1	3.2
4370	94	9	37	1071	**	**	0.5	*	*	1.4
4520	132	12	48	1406	24	0.3	3.0	0.4	0.2	6.7
4875	230	19	73	2152	**	**	0.4	*	*	3.4
4927	217	17	68	1974	48	0.3	2.1	0.5	0.4	8.3
4928	237	19	74	2215	**	**	0.5	*	*	3.5
5010	280	22	86	2584	48	0.4	2.0	0.5	0.4	9.0
5037	258	20	76	2209	48	0.3	2.0	0.5	0.4	8.8
5191	226	17	68	1921	48	0.3	6.3	0.4	0.5	7.4

All values presented in mmol/L

*Not detected

**Not analyzed for.

Table D.1. Geochemical data of brine collected at Wellington oilfield in Sumner County, Kansas.

Saturation Indices: Brine									
Depth (m)	dolomite	calcite	aragonite	kaolinite	illite	siderite	anhydrite	gypsum	Silica (am)
1277	2.99	1.05	0.91	6.25	7.03	0.81	-0.62	-0.65	-1.45
1321	2.78	0.95	0.81	6.42	7.06	0.76	-0.29	-0.33	-1.47
1332	2.06	0.56	0.42	*	*	1.08	-0.51	-0.57	-1.16
1378	1.75	0.42	0.28	8.20	9.39	0.79	-0.38	-0.49	-1.00
1486	1.39	0.26	0.12	*	*	-0.53	-0.64	-0.80	-0.99
1502	1.25	0.20	0.05	8.38	9.68	0.18	-0.64	-0.80	-1.00
1502.1	1.37	0.26	0.11	*	*	-0.46	-0.70	-0.87	-0.99
1527	-0.17	-0.51	-0.14	*	*	-0.74	-0.67	-0.87	-0.85
1535	0.22	-0.31	-0.45	8.18	9.21	-0.48	-0.72	-0.91	-0.99
1582	2.27	0.71	0.57	8.21	10.01	1.17	-0.78	-0.95	-1.03

*No Al data available to examine these phases

Table D.2. Saturation Indices of mineral species for brine collected from KGS 1-32 and KGS 1-28 drilled within Wellington oil field in Sumner County, Kansas prior to addition of the primary mineral phases in the reservoir rocks; calcite, dolomite, and pyrite, calculated using PhreeqC.

Saturation Indices: Brine equilibrated with reservoir minerals														
Depth (m)	dolomite	calcite	aragonite	pyrite	kaolinite	illite	siderite	ferrihydrite	anhydrite	gypsum	Silica (am)	hematite	goethite	jarosite
1277	0	0	-0.14	0	6.92	6.97	-5.31	-10.06	-0.53	-0.56	-1.44	-9.27	-5.17	-32.99
1321	0	0	-0.14	0	6.83	6.63	-5.53	-10.61	-0.18	-0.22	-1.46	-10.4	-5.74	-33.29
1332	0	0	-0.14	0	*	*	0.41	-4.29	-0.34	-0.41	-1.15	2.23	0.57	-14.6
1378	0	0	-0.14	0	7.86	8.38	0.27	-4.45	-0.22	-0.33	-0.99	1.87	0.38	-14.67
1486	0	0	-0.14	0	*	*	-0.89	-5.66	-0.48	-0.64	-0.98	-0.53	-0.84	-18.8
1502	0	0	-0.14	0	8.21	9.09	-0.12	-4.47	-0.49	-0.65	-1	1.83	0.34	-15.87
1502.1	0	0	-0.14	0			-0.81	-5.52	-0.54	-0.71	-0.99	-0.26	-0.71	-18.59
1527	0	0	-0.14	0			-0.33	-4.84	-0.51	-0.71	-0.86	1.11	-0.03	-16.72
1535	0	0	-0.14	0	8.33	9.9	-0.78	-4.52	-3.47	-3.66	-1.01	1.73	0.29	-23.67
1582	0	0	-0.14	0	8.59	9.9	0.28	-3.71	-3.07	-3.25	-1.02	3.32	1.08	-19.9

*No Al data available to examine these phases

Table D.3. Saturation Indices of mineral species for brine collected from KGS 1-32 and KGS 1-28 drilled within Wellington oil field in Sumner County, Kansas after the equilibration with the primary mineral phases in the reservoir rocks; calcite, dolomite, and pyrite, calculated using PhreeqC.